Modelling of immiscible WAG with emphasis on the effect of capillary pressure

Elisabeth Iren Dale

Dissertation for the degree philosophiae doctor (PhD)

at the University of Bergen

2008

Elisabeth Iren Dale
Centre for Integrated Petroleum Research
Department of Physics and Technology
University of Bergen
Allégaten 41
N-5007 Bergen
Norway

Bergen, Norway
2008

Preface

This dissertation was submitted for the degree Philosophiae Doctor at the University of Bergen. The dissertation consists of seven papers and an introduction including theoretical background. The papers are based on work done in the period 2004 to 2007 at the Centre for Integrated Petroleum Research at the University of Bergen.

The subject of this thesis is parameters governing three-phase flow in porous media with a special emphasis on the effect of capillary pressure. The effects of different parameters on flow and the relation between these parameters have been studied. The effect of capillary pressure on flow has been studied for both two-and three-phase cases. How three-phase capillary pressure differs from two-phase capillary pressure was investigated, and representations of three-phase capillary pressures were described.

Acknowledgements

I would like to thank my supervisor Professor Arne Skauge for helpful discussions and guidance.

I would also like to thank family, friends and colleagues for their support.

The financial support for this project was provided by StatoilHydro ASA.

List of papers

1. Dale, E. I., and Skauge, A.: "Fluid Flow Properties of WAG Injection Processes", paper for the 13th European Symposium on Improved Oil Recovery, Budapest, Hungary, 25. – 27. April 2005.

2. Dale, E. I., and Skauge, A.: "Features Concerning Capillary Pressure and the Effect on Two-Phase and Three-Phase Flow", paper for the 14th European Symposium on Improved Oil Recovery, Cairo, Egypt, 22. – 24. April 2007.

3. Dale, E. I., and Skauge, A.: "Influence of Capillary Pressure on Estimation of Relative Permeability for Immiscible WAG Processes", to be submitted to Journal of Petroleum Science and Engineering.

4. Dale, E. I., and Skauge, A.: "Effect of implementing three-phase flow characteristics and capillary pressure in simulation of immiscible WAG", to be submitted.

5. Dale, E. I., van Dijke, M. I. J., and Skauge, A.: "Prediction of Three-Phase Capillary Pressure Using a Network Model Anchored to Two-phase Data", submitted to Transport in Porous Media.

6. Holm, R., Kaufmann, R., Dale, E. I., Aanonsen, S., Fladmark, G., Espedal, M., and Skauge, A.: "Creating Three-Phase Capillary Pressure Functions by Parameter Matching using a Modified Ensemble Kalman Filter", submitted to special volume in Communications in Computational Physics (CiCP): Computational Methods in Energy and Environmental Research, 2008.

7. Skauge, A., and Dale, E. I.: "Progress in Immiscible WAG Modelling", SPE 111435, paper for the 2007 SPE/EAGE Reservoir Characterization and Simulation Conference, Abu Dhabi, U.A.E., 28. – 31. October 2007.

Contents

Papers

1. Introduction

Three-phase flow of gas, oil and water is common in petroleum reservoirs, especially because of use of water-alternating-gas injection (WAG). It is important to describe three-phase flow behaviour in porous media as accurately as possible. This will lower the risk of making wrong decisions.

Identifying the parameters governing three-phase flow in porous media is essential. The relation between these parameters is also important to find. These issues are addressed in this work.

Capillary pressure is in many cases neglected in reservoir simulators. This could be due to lack of measured data or the belief that the capillary pressure only has insignificant effect on the flow behaviour. This work tries to show the effect of capillary pressure on flow. The effect of capillary pressure on estimation of relative permeability and differential pressure has been studied.

The effect of three-phase characteristics and capillary pressure on the size of the three-phase area, breakthrough time of the injected fluids and oil recovery has been investigated. The features considered are three-phase representations of relative permeability, effect of trapped gas on residual oil, and capillary pressure effects.

Three-phase capillary pressure is poorly understood. It is very difficult to measure three-phase capillary pressure. Two-phase capillary pressure or models for the three-phase capillary pressure is often used as input to three-phase flow simulators. In this work the three-phase capillary pressure was predicted using a network model anchored to experimentally measured two-phase data.

This thesis consists of two parts; the first part presents a theoretical background for the work, and the second part is a collection of papers.

Chapter 2 to 7 of the theoretical background includes definitions and descriptions of wettability, interfacial tension, spreading, capillary pressure, hysteresis and relative permeability. Background for the network model used is presented in chapter 8. Chapter 9 describes three-phase modelling in the simulator Eclipse 100. A summary of the main results are given in chapter 10. Further work is discussed in chapter 11.

Seven papers are included. The titles of the papers are “Fluid Flow Properties of WAG Injection Processes”, “Features Concerning Capillary Pressure and the Effect on Two-Phase and Three-Phase Flow”, “Influence of Capillary Pressure on Estimation of Relative Permeability for Immiscible WAG Processes”, “Effect of implementing three-phase flow characteristics and capillary pressure in simulation of immiscible WAG”, “Prediction of Three-Phase Capillary Pressure Using a Network Model Anchored to Two-phase Data”, “Creating Three-Phase Capillary Pressures by Parameter Matching using a Modified Ensemble Kalman Filter” and ”Progress in Immiscible WAG Modelling”.

2. Wettability

2.1 Definition

Wettability describes the fluids tendency to spread on a surface in the presence of other immiscible fluids. It is a measure of which phase preferentially adheres to a surface. When two immiscible phases, i.e. oil and water, is in contact with a rock surface the contact angle between the two fluids determines the wettability of the rock. The contact angle, θ_{ow}, is by convention measured through the denser fluid, in this case the water phase, see figure 2.1. If the angle is between 0º and 60º to 75º the rock is defined as water-wet, if the angle is between 105º to 120º and 180º the rock is defined as oil-wet and if the angle is between these ranges, close to 90º, the rock is considered to have neutral or intermediate wettability.[1-5]

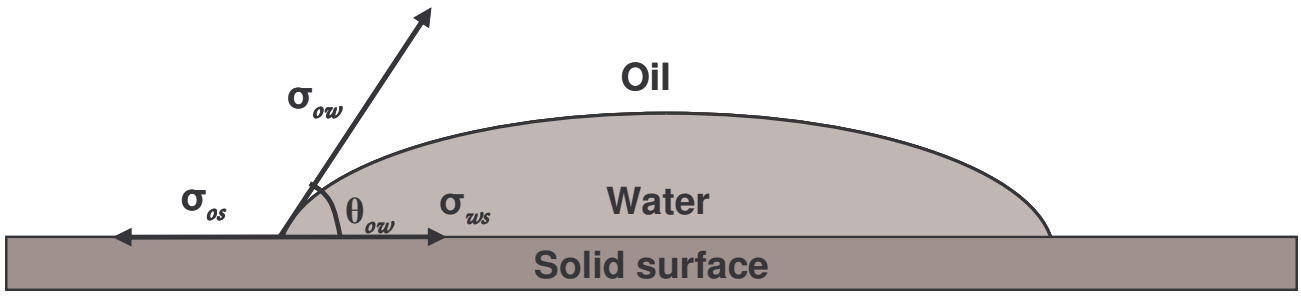

Figure 2.1: A drop of water spreading on a solid surface.

2.2 Intermediate wettability classes

The intermediate wettability state is often divided into two classes; fractionally-wet and mixed-wet. Fractionally wet porous media have oil-wet and water-wet pores randomly distributed in the different pore sizes, see figure 2.2 a). In the mixed-wet case the oil-wet and water-wet pores are distributed by pore size. When the large pores are oil-wet and the small pores are water-wet it is called a mixed-wet large

state, see figure 2.2 b). Mixed-wet small is the case when the small pores are oil-wet and the large pores are water-wet, see figure 2.2 c).

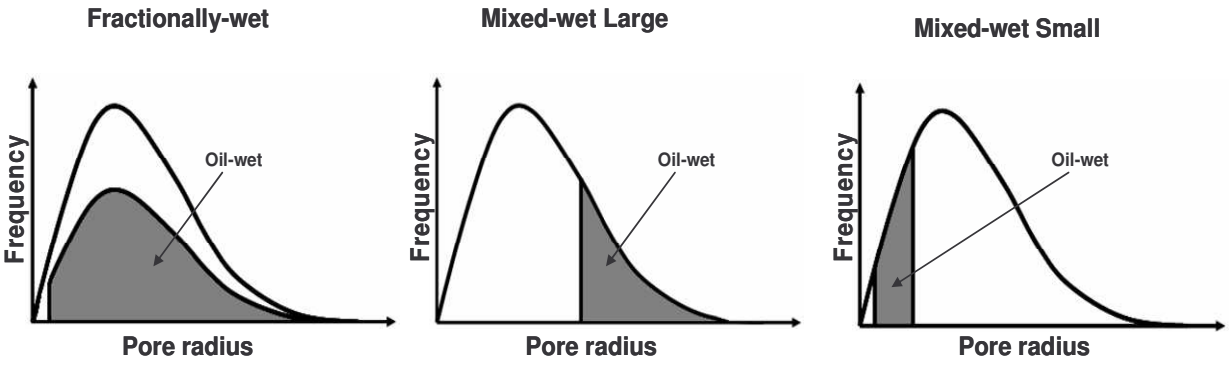

a) b) c)

Figure 2.2: Distribution of oil-wet pores for a) fractionally-wet, b) mixed-wet large and c) mixed-wet small systems.

3. Interfacial tension

3.1 Definition

When two immiscible fluids, like oil and water, are in contact there exists a surface between them. The molecules near this surface have different degrees of attractions to their neighbouring molecules. This produces a free surface energy per. surface unit, called interfacial tension. If the fluids are a gas and a liquid the forces acting on the interface is called surface tension. The interfacial or surface tension is usually denoted using the symbol σ. The interfacial tension between oil and water, σ_{ow}, is shown in figure 2.1. The energy barrier produced by interfacial tension prevents one liquid from becoming emulsified into the other.[2-3,5-6]

3.2 The presence of a solid surface

The Young-Dupre equation follows from the force balance and is given by[2,5]

$$\sigma_{os} - \sigma_{ws} = \sigma_{ow} \cos\theta_{ow}, \qquad (1)$$

where σ_{os} is the interfacial tension between the oil and the solid , σ_{ws} is the interfacial tension between the water and the solid, σ_{ow} is the interfacial tension between the oil and the water and θ_{ow} is the angle between the interface and the solid.

In three-phase flow three contact angles are involved, the angle between the oil-water surface and the solid, between the gas-water surface and the solid and between the gas-oil surface and the solid. An expression for the relationship between the different contact angles in the three-phase case can be found by combining the force balance for the three cases seen in figure 3.1

$$\sigma_{os} - \sigma_{ws} = \sigma_{ow} \cos\theta_{ow}, \tag{2}$$

$$\sigma_{gs} - \sigma_{ws} = \sigma_{gw} \cos\theta_{gw} \text{ and} \tag{3}$$

$$\sigma_{gs} - \sigma_{os} = \sigma_{go} \cos\theta_{go}. \tag{4}$$

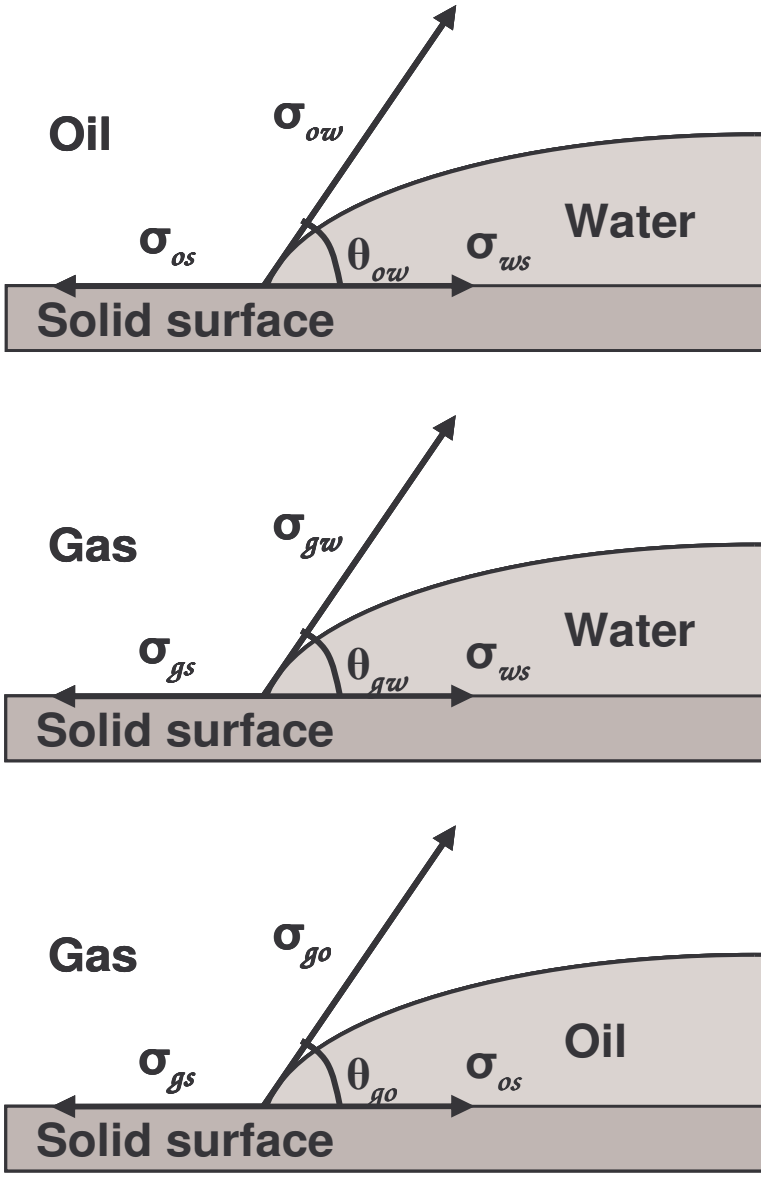

Figure 3.1: Force balance of fluid-solid combinations for three-phase flow.

When these three relations are combined we get the Bartell-Osterhof equation[7]

$$\sigma_{gw}\cos\theta_{gw} = \sigma_{ow}\cos\theta_{ow} + \sigma_{go}\cos\theta_{go}. \quad (5)$$

3.3 Forces in a capillary tube

If a tube is lowered into water the surface tension and wettability will cause the water to rise inside the tube to a higher level than outside. The water will rise to the height where the capillary forces are balanced by the weight of the water column[6], see figure 3.2.

The upward force is given by

$$F_{up} = (2\pi r)\sigma_{aw}\cos\theta_{aw}, \quad (6)$$

where σ_{aw} is the surface tension between air and water, θ_{ow} is the contact angle and r is the radius of the tube. The downward force is given by

$$F_{down} = \pi r^2 h(\rho_w - \rho_a)g, \quad (7)$$

where h is the height the water rises in the capillary tube, ρ_w is the density of water, ρ_a is the density of air and g is the gravity acceleration.

If we assume that the density of air is negligible when compared to the density of water the surface tension is given by

$$\sigma_{aw} = \frac{r\,h\,\rho_w\,g}{2\cos\theta_{aw}}. \quad (8)$$

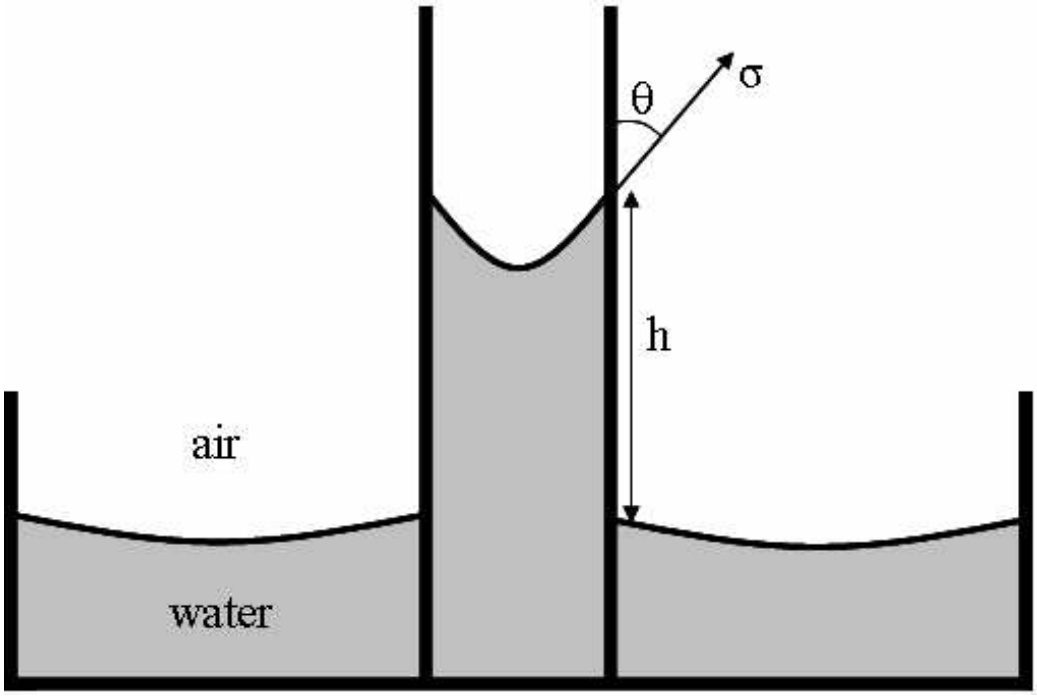

Figure 3.2: Capillary tube (Adapted from Ahmed[6]).

4. Spreading

4.1 Definition

When three fluids are in contact there may be formed a three-phase contact line between the fluids. In figure 4.1 a) a lens of one of the fluids is formed on the contact surface of the two other fluids. In other cases one of the fluids will spread as a layer separating the two other fluids, as seen in figure 4.1 b).

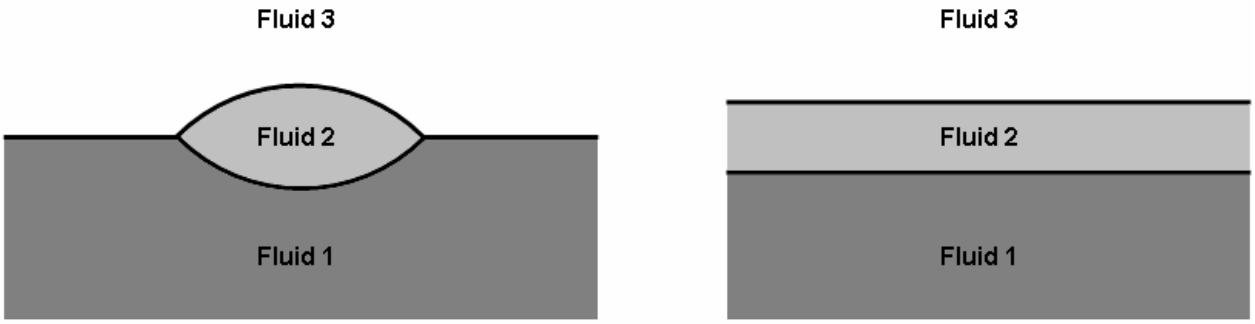

Figure 4.1: a) Non-spreading system *b) Spreading system*

4.2 Force balance

Figure 4.2 shows a contact line formed between gas, oil and water. A lens of oil is resting on the gas-water interface. The gas-water interfacial tension is denoted σ_{gw}, the gas-oil interfacial tension is denoted σ_{go} and the oil-water interfacial tension is denoted σ_{ow}. The angle between the gas-oil and oil-water interface is denoted θ_{go} and the angle between the gas-water and oil-water interface is denoted θ_{ow}.

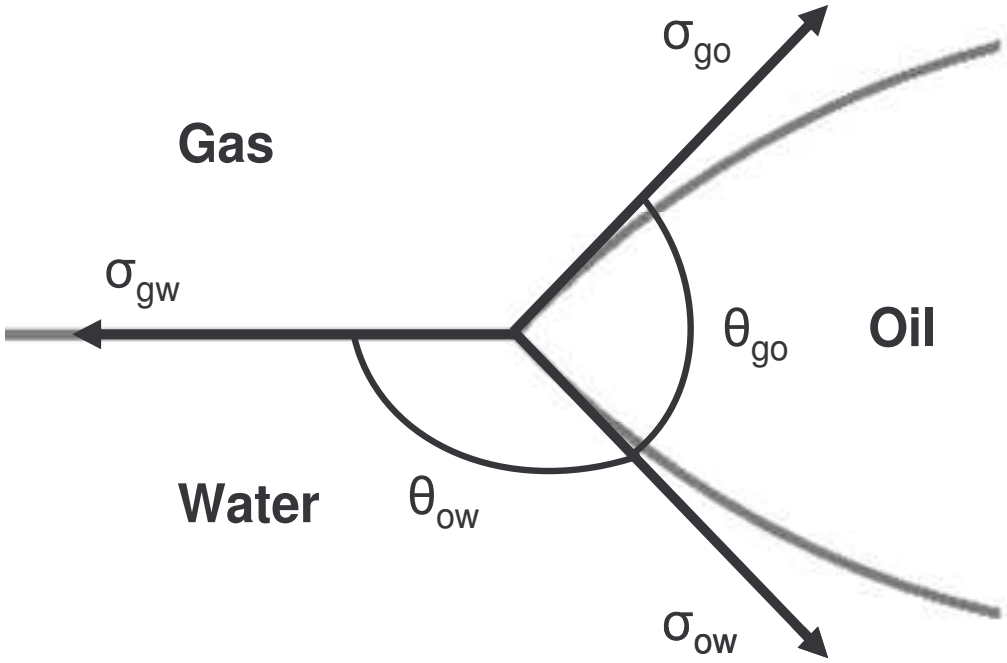

Figure 4.2: Contact line between gas, oil and water.

To get equilibrium the equation

$$\sigma_{gw} = \sigma_{ow}\cos\theta_{ow} + \sigma_{go}\cos\theta_{go} \tag{9}$$

has to be satisfied. This is the case when $\sigma_{gw} < (\sigma_{ow} + \sigma_{go})$. A lens of oil will then be formed in the gas-oil-water system. If $\sigma_{gw} > (\sigma_{ow} + \sigma_{go})$ the condition for equilibrium is not satisfied, and the oil will spread as a layer between the gas and the water.[2]

The spreading coefficient is defined as

$$C_{s,o} = \sigma_{gw} - \sigma_{ow} - \sigma_{go} \ . \tag{10}$$

If $C_{s,o}$ is equal to zero the oil is spreading and if the coefficient is less than zero the oil is non-spreading.

5. Capillary pressure

5.1 Definition

The difference in pressure across a curved boundary between two immiscible fluids is called capillary pressure. The capillary pressure is defined as the pressure in the non-wetting phase minus the pressure in the wetting phase[1-5,8]

$$P_C = P_{non-wetting} - P_{wetting} \,. \tag{11}$$

The capillary pressure between e.g. oil and water, where water is the wetting phase, is thus defined as

$$P_C = P_{oil} - P_{water} \,. \tag{12}$$

The capillary pressure is dependent on the interfacial tension between the fluids and the rock, the geometry of the pores and the wettability[6].

5.2 Capillary pressure in a capillary tube

The capillary pressure between air and water at static conditions in a capillary tube can be expressed as

$$P_{C,aw} = \frac{F_{down}}{A} = h(\rho_w - \rho_a)g \,, \tag{13}$$

where F_{down} is the downward forces in the capillary tube, A is the cross section area of the tube, h is the height the water rises in the capillary tube, ρ_w is the density of water, ρ_a is the density of air and g is the gravity acceleration.

In general the capillary pressure is given as[6]

$$P_C = \Delta\rho\, g\, h\,. \tag{14}$$

5.3 The Young-Laplace equation

An expression for calculating the capillary pressure across curved surfaces is provided by the Young-Laplace equation[9-10]

$$P_C = \sigma\left(\frac{1}{R_1}+\frac{1}{R_2}\right), \tag{15}$$

where P_C is the capillary pressure, σ is the interfacial tension, and R_1 and R_2 is the main radii of curvature for the surface. A curved surface is described by the two radii of curvature, R_1 and R_2, seen in figure 5.1.[3,5]

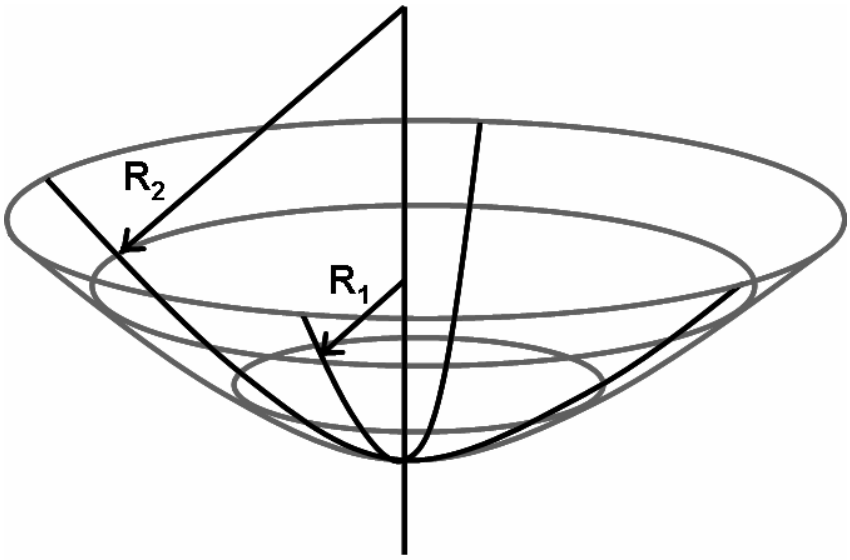

Figure 5.1: The principal radii of curvature, R_1 and R_2 (Adapted from Zolotukhin and Ursin[5]).

5.4 Cylindrical tube

If we consider a pore to be a straight cylindrical tube with radius r, the surface between the two fluids is approximated by a sphere surface, see figure 5.2. (This is not entirely accurate because the surface curves more near the walls of the tube.) The radius of curvature between the two fluids is then $R_1 = R_2 = R$, [3,5,8] and

$$R = \frac{r}{\cos\theta}. \tag{16}$$

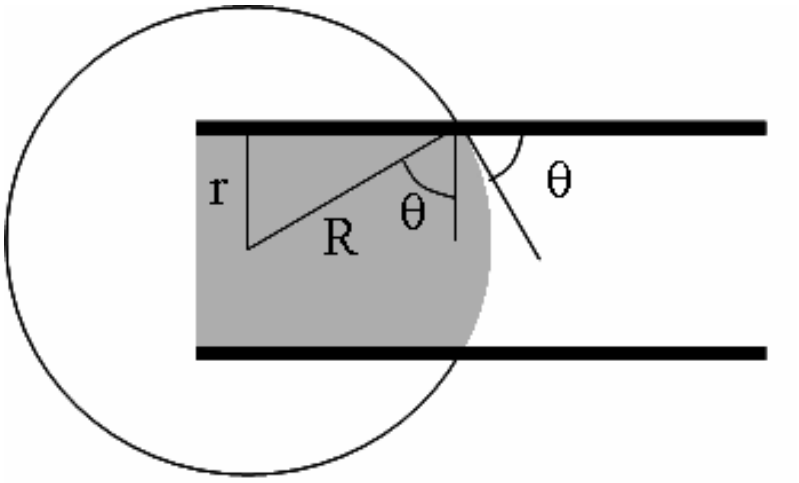

Figure 5.2: A straight cylindrical tube containing two fluids.

The capillary pressure for a cylindrical tube of radius r can therefore be written as

$$P_C = \frac{2\sigma\cos\theta}{r}. \tag{17}$$

5.5 Capillary pressure curve - connection with saturation

It is evident from equation 15 that the capillary pressure is proportional to the inverse of the radii of curvature. The saturation of the different fluids will affect the radii of curvature. If we consider a water-wet reservoir we find that if the water saturation declines the radii of curvature is also reduced, as seen from figure 5.3. The conclusion is therefore that there must be an inverse connection between the capillary pressure and the water saturation for a water-wet reservoir. For reservoirs with other wettabilities the argumentation will be similar.[3,5]

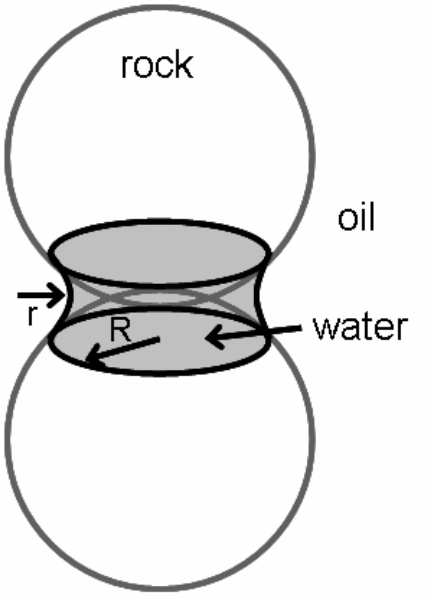

Figure 5.3: Water between two sand grains in a water-wet reservoir (Adapted from Zolotukhin and Ursin[5]).

When the saturation of the wetting fluid is decreasing it is called a drainage process. A typical capillary pressure curve for drainage in the case of two-phase flow of oil and water is seen in figure 5.4. The minimum capillary pressure needed to start the invasion of oil in the porous medium is called the capillary entry pressure, P_e, and is

seen in figure 5.4. The capillary pressure increases as the water saturation decreases and goes towards infinity at the irreducible water saturation, S_{wi}.

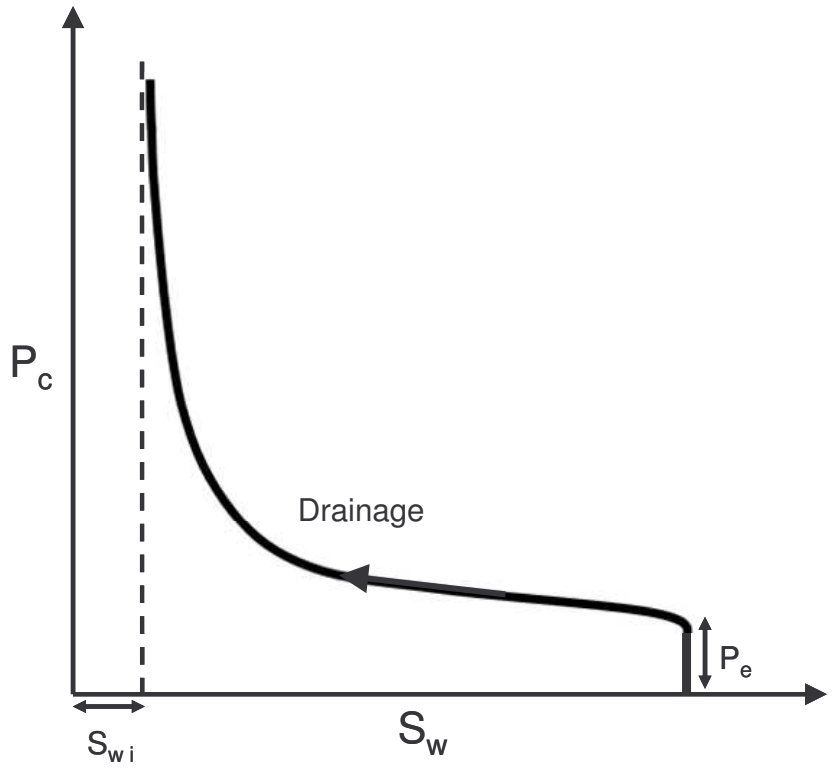

Figure 5.4: Capillary pressure curve.

5.6 Drainage and imbibition - capillary pressure hysteresis

Drainage is the process where the non-wetting fluid displaces the wetting fluid, and imbibition is the process where the wetting fluid displaces the non-wetting fluid. Primary drainage is the process where oil is forced into the oil-water system by increasing the oil pressure, between point 1 and 2 in figure 5.5.

When decreasing the oil pressure after primary drainage the capillary pressure will decrease, and the water will spontaneously enter the rock, between point 2 and 3. This spontaneous imbibition will stop when the capillary pressure reaches zero, point 3. In order to increase the water saturation further the pressure in the water phase has

to be increased. The capillary pressure will get a more and more negative value, between point 3 and 4. This is called forced imbibition. When the residual oil saturation is reached the capillary pressure goes towards minus infinity.

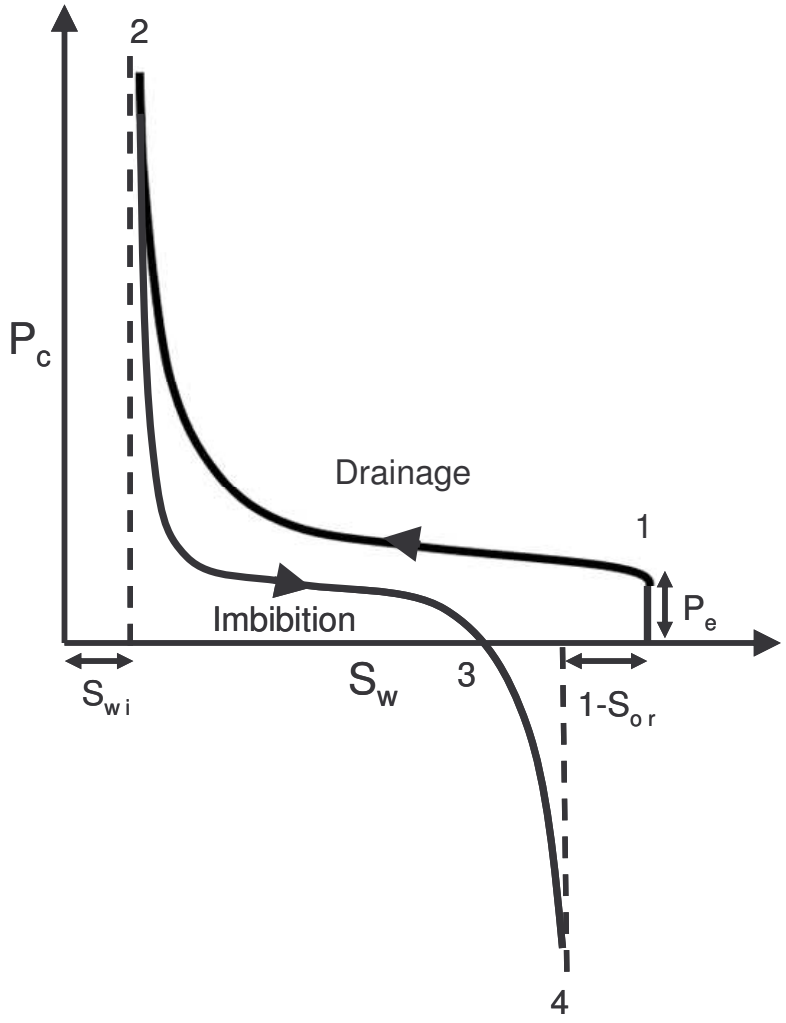

Figure 5.5: Drainage and imbibition.

Because of hysteresis effects, the capillary pressure is different for drainage and imbibition[1], see figure 5.5. The imbibition capillary pressure is lower than the drainage capillary pressure at the same saturation value. The cause of hysteresis effects is discussed in chapter 6.

5.7 Influence of pore size distribution

The pore size distribution will have a large effect on the shape of the capillary pressure curve. If the capillary pressure is given by

$$P_C = \frac{2\sigma \cos\theta}{r}, \tag{18}$$

it is evident that a large pore radius will give low capillary pressure and a small pore radius will give high capillary pressure. In a drainage situation the largest pores will be invaded first and then the invasion will continue through smaller and smaller pores.

The entry pressure is given by

$$P_e = \frac{2\sigma \cos\theta}{r_{\max}}, \tag{19}$$

where $r_{\max}$ is the maximum pore size in the porous medium. A high maximum pore radius, as seen in case 2 in figure 5.6, will give a low capillary entry pressure as seen in figure 5.7. If the maximum pore radius is higher, as in case 1, the entry pressure will be higher.

If the porous medium is well sorted, case 1 in figure 5.6, the capillary pressure will be almost flat in the middle section of the curve. In this case many pores are invaded at the same time because many pores have approximately the same size. [11] If the porous medium is poorly sorted as in case 2 the capillary pressure will have a fairly steep slope for the entire saturation range[11], as seen in figure 5.7.

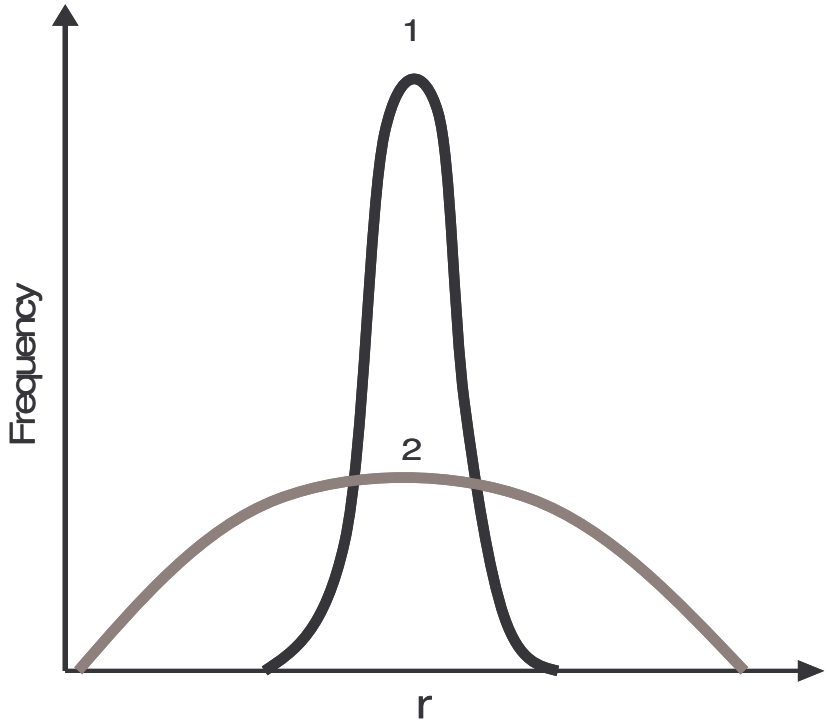

Figure 5.6: Different pore size distributions (Adapted from Selley[11]).

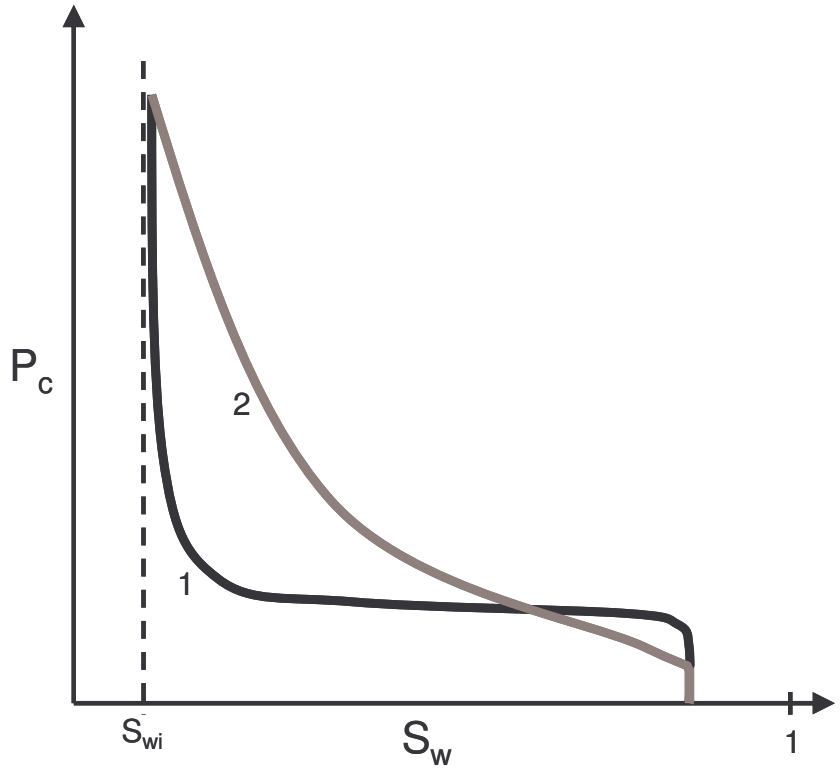

Figure 5.7: Capillary pressure for different pore size distributions (Adapted from Selley[11]).

5.8 Influence of wettability

The wettability of the rock will have a large effect on the capillary pressure curve.

When the rock is strongly water wet, a large amount of work is required for the drainage process where the wetting fluid is displacing the non-wetting fluid, see figure 5.8. Little or no work is required during imbibition, when the wetting fluid is displacing the non-wetting fluid. The wetting fluid will spontaneously imbibe into the strongly water-wet rock.

Also for a strongly oil-wet rock a large amount of work must be used to drain the wetting fluid, see figure 4.8. In this case the wetting fluid is oil, and the capillary pressure is often defined as negative when the water has the highest pressure, see eq. 12. Oil imbibes spontaneously into the strongly oil-wet rock until zero capillary pressure is reached.

For intermediate-wet cases some work is required in both the drainage and imbibition process, because the rock has no preference for either one of the fluids, see figure 5.8. Some of the water imbibes spontaneously into the core. When increasing the water pressure more water can be forced into the core. The forced imbibition has a negative capillary pressure value.[12]

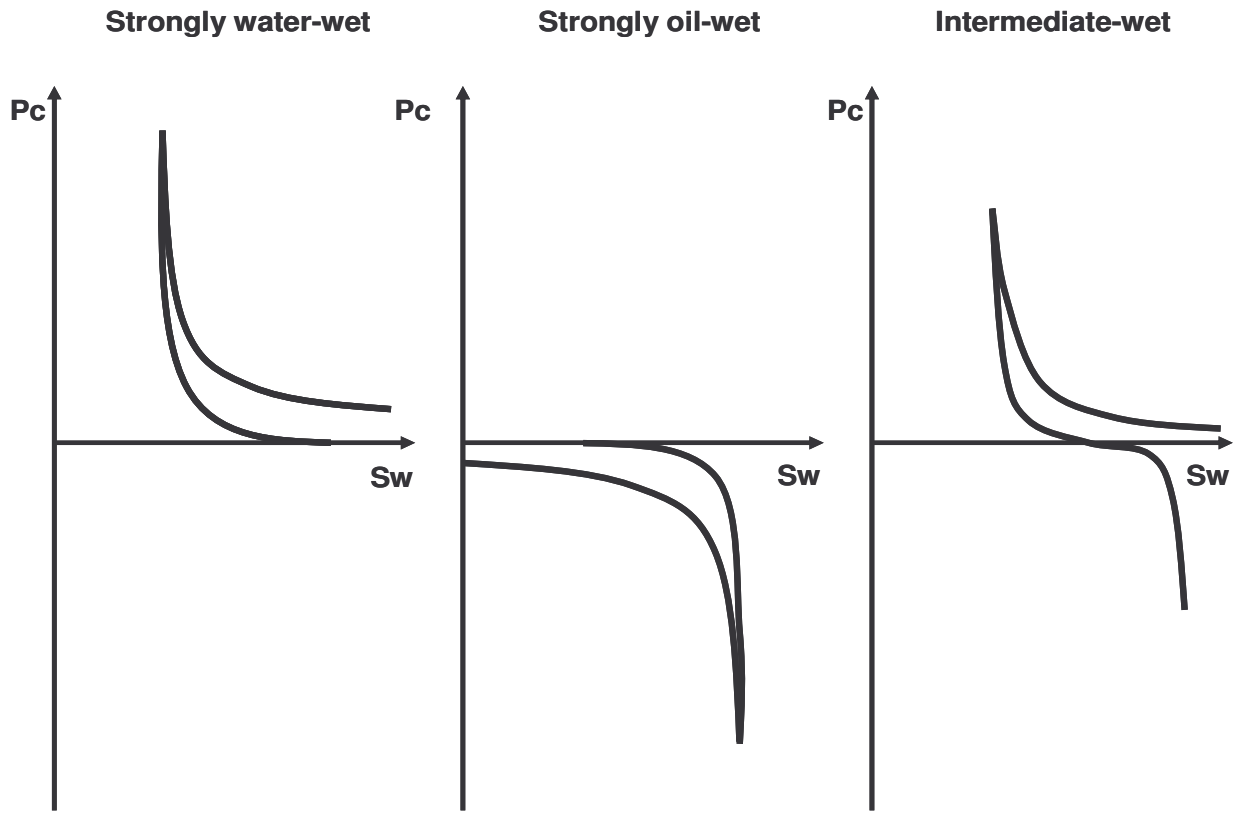

Figure 5.8: Capillary pressure for different wettability (Adapted from Killins[12]).

5.9 Capillary pressure correlations for two-phase flow

Correlations for capillary pressure describe the relationship between capillary pressure and saturation.[13-22] One of the best-known correlations is the Brooks and Corey equation[13], where the capillary pressure is a function of the effective saturation

$$P_C = P_C(S_e), \tag{20}$$

where the effective saturation is expressed as

$$S_e = \frac{S_w - S_{wi}}{1 - S_{wi}}. \tag{21}$$

S_w is the water saturation and S_{wi} is the irreducible water saturation. The correlation is given as

$$S_e = \left(\frac{C}{P_C} \right)^2 , \tag{22}$$

where C is a constant. Based on this work Standing[14] formulated the expression

$$S_e = \left(\frac{P_e}{P_C} \right)^{\lambda} , \tag{23}$$

where P_e is the capillary entry pressure and λ is a pore size index.

Skjæveland et al.[15] found an expression for mixed wettability based on the Brooks and Corey correlation. The capillary pressure is given as

$$P_C = \frac{c_w}{\left(\frac{S_w - S_{wi}}{1 - S_{wi}} \right)^{a_w}} + \frac{c_o}{\left(\frac{S_o - S_{or}}{1 - S_{or}} \right)^{a_o}} , \tag{24}$$

where a and c are constants.

5.10 Capillary pressure correlations for three-phase flow

Killough's method is often used to model three-phase capillary pressure[23]. The three-phase capillary pressure is constructed as a weighted average between the two-phase drainage and imbibition curves[24]

$$P_C = P_{Cd} + F\left(P_{Ci} - P_{Cd}\right) \tag{25}$$

and F given by

$$F = \frac{\left(\frac{1}{S_w - S_{w,hys} + E} - \frac{1}{E}\right)}{\left(\frac{1}{S_{w,\max} - S_{w,hys} + E} - \frac{1}{E}\right)}, \tag{26}$$

where P_{Cd} is the drainage capillary pressure, P_{Ci} is the imbibition capillary pressure, $S_{w,hys}$ is the water saturation at the hysteresis reversal point, $S_{w,\max}$ is the maximum water saturation attainable on the scanning curve when trapping of the other phases is subtracted and E is a curvature parameter. Figure 5.9 show the three-phase scanning curves and the two-phase drainage and imbibition curves.

Helland and Skjæveland[25] proposed a correlation for three-phase capillary pressure. This analytical function depends on the direction of saturation change. The input parameters have to be determined by matching to three-phase experiments.

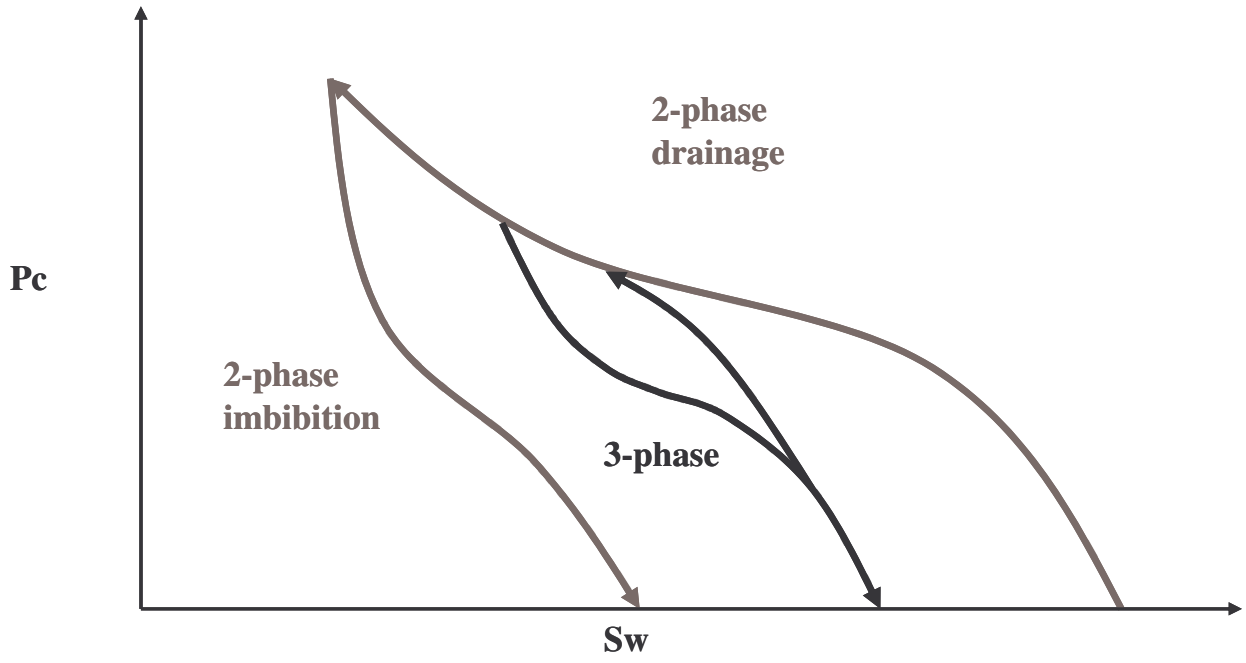

Figure 5.9: Capillary pressure for three-phase flow (Adapted from Eclipse technical description[26]).

Very few measurements of three-phase capillary pressure exist.[27-28] Kalaydjian[27] measured three-phase capillary pressure on an outcrop water-wet core and on unconsolidated material. The capillary pressure was a function of all three saturations for both drainage and imbibition. The three-phase capillary pressure had a higher value than the two-phase capillary pressure. This would indicate that Killough's correlation[23] could not be used to predict three-phase capillary pressure.

5.11 Three-phase capillary pressure from network modelling

A network model is a representation of the pore space geometry, and incorporates the physical rules of flow inside the pores. As we are getting closer to describing the microscopic flow satisfactorily the development of truly predictive models is possible. A large range of transport phenomena can be studied by use of network models.[29]

A few attempts have been made to estimate three-phase capillary pressure using network models.[30-33] The network models are usually anchored to measured two-phase capillary pressure data and three-phase capillary pressure is predicted. For more details on network modelling see chapter 8 and 10.

6. Hysteresis

6.1 Definition

The irreversibility of the fluid flow processes is called hysteresis. Capillary pressures and relative permeabilities are history dependent. The have different values depending on whether a fluid saturation is increasing or decreasing.

Several things may cause hysteresis. The main causes are contact angle hysteresis, pore geometry and trapping of fluids.

6.2 Contact angle hysteresis

The interfacial tensions and the contact angles between the fluids may be different for advancing, θ_a, and receding cases, θ_r, as seen in figure 6.1. Advancing contact angles are larger than the receding contact angles.

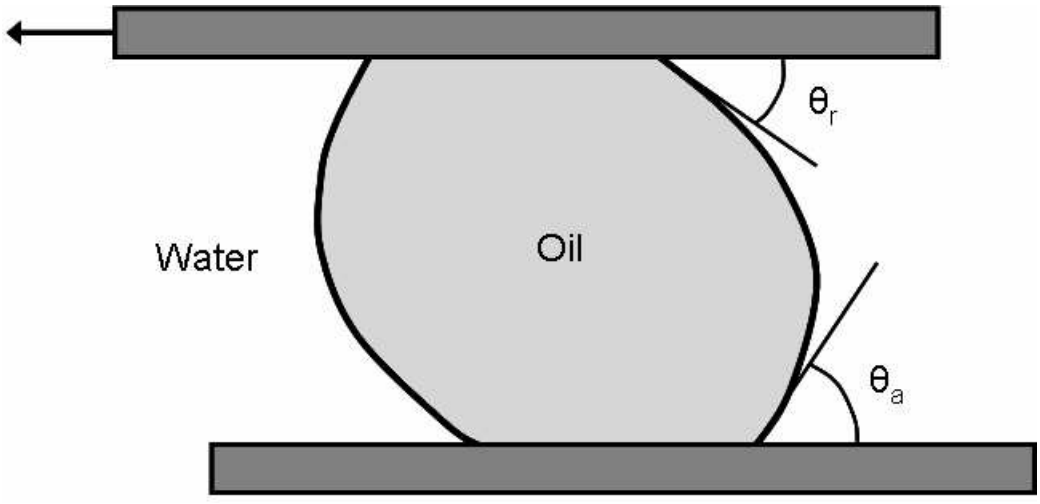

Figure 6.1: Contact angle Hysteresis (Adapted from Zolotukhin and Ursin[5]).

Contact angle hysteresis could be caused by contamination of the liquid or the solid, surface roughness, or surface immobility on a macromolecular scale.[34]

6.3 Trapping

Hysteresis can also be caused by trapping. During a flooding process phases can be trapped in the porous medium causing the process to be irreversible. Two models explaining the trapping mechanism is the pore doublet model and the snap-off model.

The pore-doublet model explains how fluids can be trapped when the fluids flow at different speeds through pores of different sizes.[35-36] The capillary forces will pull the wetting fluid into the small pores, but the viscous forces will give a higher speed through the large pores. The competition between these two forces will lead to trapping in either the small or large pores. Figure 6.3 illustrates a process with low injection rate dominated by capillary forces. The wetting phase flows at a larger speed through the smaller pores, and the non-wetting phase is trapped in the larger pores.

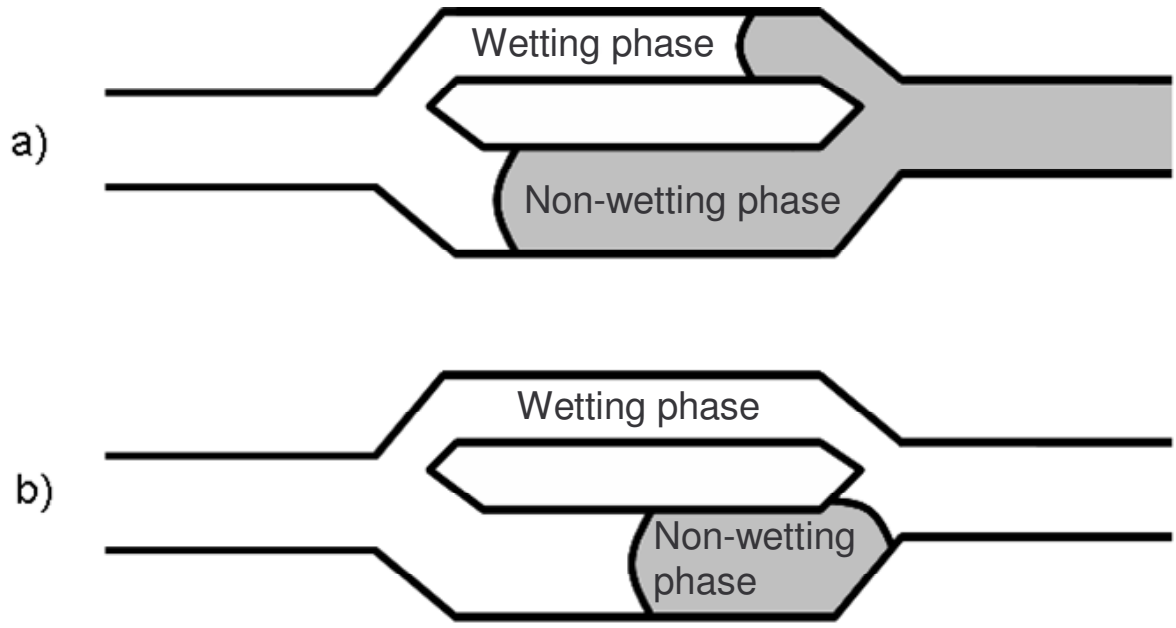

Figure 6.3: Pore doublet model; a) before trapping and b) after trapping.

The snap-off model explains how fluid can be trapped if the aspect ratio, the relation between the size of the pore body and the pore throat, is high.[6] In water-wet pores the oil can be trapped if the collar of water in the pore throat expands and meets in the middle, as seen in figure 6.4. The oil in the pore is then no longer connected to the rest of the oil-phase and cannot escape from the pore.

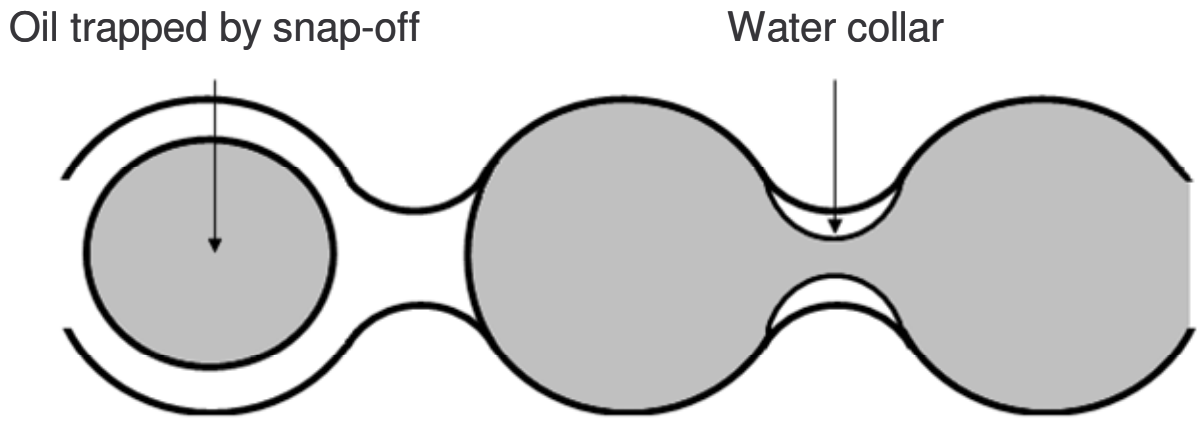

Figure 6.4: Snap-off model (Adapted from Chatzis et. al[36]).

7. Relative permeability

7.1 Definition

The permeability of a porous medium quantifies the ability of the medium to transport fluids through the pores. In Darcy's law[37] the permeability is considered to be a constant value, k. This is true if the porous media is completely saturated with one fluid. This parameter is called the absolute permeability. The Darcy equation for horizontal flow of an incompressible fluid is given as

$$q = \frac{kA}{\mu}\left(\frac{dP}{dx}\right), \tag{27}$$

where q is the flow rate, k is the absolute permeability, A is the cross-section area of the porous medium, μ is the viscosity of the fluid, dP is the differential pressure and dx is the differential length of the porous medium.

If more than one fluid is present the flowing capability of each fluid is described by an effective permeability. The sum of the effective permeability values is often less than the absolute permeability, and sometimes the sum is higher than the absolute permeability. The relative permeability for each of the fluids is expressed as the relation between effective permeability and the absolute permeability. The relative permeability for fluid i is written as

$$k_{ri} = \frac{k_i}{k}, \tag{28}$$

where k_i is the effective permeability for fluid i and k is the absolute permeability.

The relative permeability of oil and water plotted against water saturation is seen in figure 7.1. At water saturations below the irreducible value, S_{wi}, the water is immobile and the relative permeability to water is zero. The relative permeability of

water increases towards the maximum water saturation. The relative permeability of oil is zero at the residual oil saturation and increases towards lower water saturation i.e. higher oil saturation.

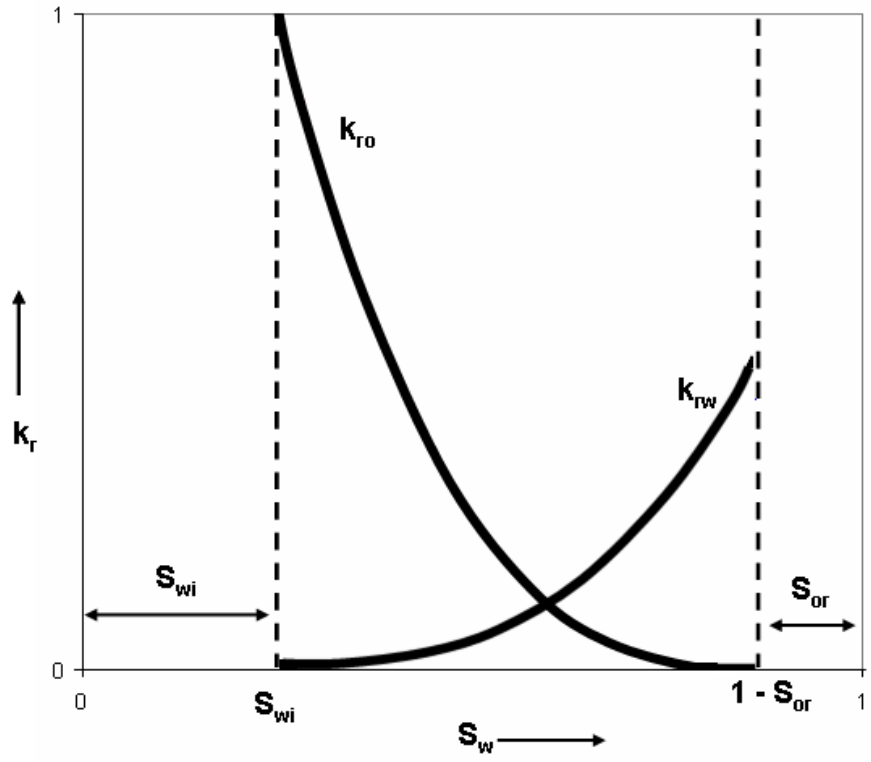

Figure 7.1: Relative permeability curves for oil and water.

7.2 Relative permeability hysteresis

Hysteresis effects are also found for relative permeability as well as for capillary pressure. Relative permeability is also direction dependent; it has different values for a saturation depending on whether the saturation increases or decreases.

Figure 7.2 shows hysteresis for oil and water relative permeability in a water wet rock. At point A we have 100 % water saturation. Between point A and B primary drainage, oil flooding, is performed. The solid lines are the relative permeability curves for the drainage process. After drainage an imbibition process, water flooding,

occurs between point B and C. The dashed lines are the relative permeability curves for the imbibition process. The relative permeability curves for the imbibition process are different from the curves from the drainage process. The initial state of 100 % water saturation is not reached after imbibition due to capillary trapping of oil. The hysteresis effect is in general more substantial in the non-wetting phase.[38]

The two dominating causes for hysteresis are, as described in chapter 6, differences in the contact angles and trapping of phases.

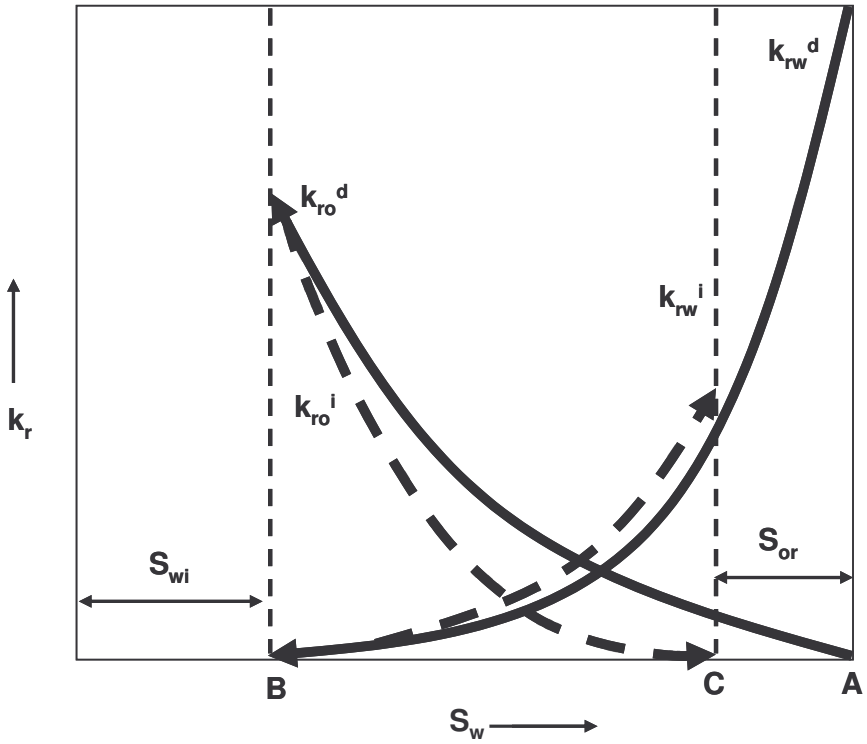

Figure 7.2: Hysteresis in relative permeability (Adapted from Bennion et. al[38]).

7.3 Relative permeability correlations for two-phase flow

Empirical correlations for relative permeability are an important tool for creating relative permeability curves when no laboratory data is available. If relative permeability is used as a history matching parameter in reservoir simulation, the

correlations make it easier to change the relative permeability between each run. One of the most well known relative permeability correlations is the Corey model[39].

For a gas-oil system he expressed the relative permeability of oil as

$$k_{ro} = \left(1 - S_g^*\right)^4 \tag{29}$$

and the relative permeability of gas as

$$k_{rg} = (S_g^*)\left(2 - S_g^*\right) \ , \tag{30}$$

where

$$S_g^* = \frac{S_g}{1 - S_{wi}}, \tag{31}$$

S_g is the gas saturation and S_{wi} is the irreducible water saturation.

For an oil-water system he expressed the relative permeability of oil as

$$k_{ro} = \left(\frac{1 - S_w}{1 - S_{wi}}\right)^4 \tag{32}$$

and the relative permeability of water as

$$k_{rw} = \left(\frac{S_w - S_{wi}}{1 - S_{wi}}\right)^4 , \tag{33}$$

where S_w is the water saturation and S_{wi} is the irreducible water saturation.

Corey's equations can only be applied to homogeneous well-sorted rocks. For other types of rocks the exponent must be changed. A more general expression for an oil-water system the water relative permeability is calculated by

$$k_{rw} = \left(S_e\right)^{a_w}, \tag{34}$$

where S_e is the effective saturation given by

$$S_e = \frac{S_w - S_{wi}}{1 - S_{wi}} \tag{35}$$

and a_w is a constant. The oil relative permeability is given by

$$k_{ro} = (1 - S_e)^{a_o}, \tag{36}$$

where a_o is a constant.

Corey-type equations are simple and easy to use. In numerical simulation analytical expressions for the relative permeabilities are often used. [6] For an oil-water system the relative permeabilities of oil and water are given as

$$k_{ro} = (k_{ro})_{S_{wi}} \left(\frac{1 - S_w - S_{orw}}{1 - S_{wi} - S_{orw}} \right)^{n_{ow}} \text{ and} \tag{37}$$

$$k_{rw} = (k_{rw})_{S_{orw}} \left(\frac{S_w - S_{wi}}{1 - S_{wi} - S_{orw}} \right)^{n_w}, \tag{38}$$

where $(k_{ro})_{S_{wi}}$ is the oil relative permeability at irreducible water saturation, $(k_{rw})_{S_{orwc}}$ is the water relative permeability at residual oil saturation after water injection, S_w is the water saturation, S_{wi} is the irreducible water saturation, S_{orw} is the residual oil saturation after water injection, n_{ow} is the oil relative permeability exponent and n_w is the water relative permeability exponent.

For gas-oil systems the following expressions are used for oil and gas relative permeabilities

$$k_{ro} = (k_{ro})_{S_{gc}} \left(\frac{1 - S_g - S_{lc}}{1 - S_{gc} - S_{lc}} \right)^{n_{og}} \text{ and} \tag{39}$$

$$k_{rg} = (k_{rg})_{S_{org}} \left(\frac{S_g - S_{gc}}{1 - S_{lc} - S_{gc}} \right)^{n_g}, \tag{40}$$

where $(k_{ro})_{S_{gc}}$ is the oil relative permeability at critical gas saturation, $(k_{rg})_{S_{orwg}}$ is the water relative permeability at residual oil saturation after gas injection, S_g is the gas saturation, S_{gc} is the critical gas saturation, S_{org} is the residual oil saturation after gas injection, S_{lc} is the total critical liquid saturation given as $S_{lc} = S_{wi} + S_{org}$, n_{og} is the oil relative permeability exponent and n_g is the gas relative permeability exponent.

7.4 History dependent relative permeability correlations for two-phase flow

Hysteresis is neglected in the Corey equation, but in many cases significant hysteresis effects have been seen. Trapping of the phases is one of the important parameters to describe. Land[40] suggested a relationship between the maximum saturation of the non-wetting phase and the trapped saturation of the non-wetting phase

$$\frac{1}{S_{nw,\max}} - \frac{1}{S_{nw,t}} = C, \tag{41}$$

where $S_{nw,\max}$ is the maximum saturation of the non-wetting fluid in an imbibition process, $S_{nw,t}$ is the trapped saturation of the non-wetting fluid after the imbibition process and C is called the Land constant. The Land constant will be dependent on wettability and process history and must be determined from experimental data.

Killough[41] and Carlson[42] also suggested models for two-phase drainage and imbibition hysteresis.

7.5 Relative permeability correlations for three-phase flow

When the three phases oil, water and gas are present in a porous media at the same time three-phase flow parameters must be used to describe the behaviour.

Three-phase relative permeability is difficult to measure and correlations of two-phase data are usually used to estimate the three-phase data. It is often assumed that the water and gas relative permeability is a function of its own saturation only, and two-phase relative permeabilities for water and gas can therefore be used for three-phase cases. Three-phase oil relative permeability is assumed to be a function of both gas and water saturation.

Many correlations for the oil relative permeability exists.[43-56] Several authors[57-59] have made summaries of correlations for three-phase relative permeability.

The Stone I and II models[44-45] for estimation of three-phase relative permeability are widely used. Stone introduced the normalised saturations

$$S_o^* = \frac{S_o - S_{orm}}{1 - S_{wi} - S_{orm}}, \tag{42}$$

$$S_w^* = \frac{S_w - S_{wi}}{1 - S_{wi} - S_{orm}} \text{ and} \tag{43}$$

$$S_g^* = \frac{S_g}{1 - S_{wi} - S_{orm}}, \tag{44}$$

where S_{orm} is the minimum oil saturation after gas and water injection.

In the Stone I model[44] the relative permeability of oil is defined as

$$k_{ro} = S_o^* \beta_w \beta_g . \tag{45}$$

β_w and β_g are given by

$$\beta_w = \frac{k_{row}}{1 - S_w^*} \text{ and} \tag{46}$$

$$\beta_g = \frac{k_{rog}}{1 - S_g^*}, \tag{47}$$

where k_{row} is the two-phase oil relative permeability in a oil-water system and k_{rog} the two-phase oil relative permeability in a gas-oil system.

The Stone II model[45] defines the oil relative permeability as

$$k_{ro} = (k_{row})_{S_{wi}} \left[\left(\frac{k_{row}}{(k_{row})_{S_{wi}}} + k_{rw} \right) \left(\frac{k_{rog}}{(k_{row})_{S_{wi}}} + k_{rg} \right) - (k_{rw} + k_{rg}) \right], \tag{48}$$

where $(k_{row})_{S_{wi}}$ is the relative permeability of oil at the irreducible water saturation from the two-phase oil-water system.

It is difficult to conduct a three-phase flow experiment. The number of experiments concerning three-phase flow is therefore limited, but some reported cases exist.[60-71] The experiments show a very complex behaviour. Several different results for the hysteresis behaviour of gas, water and oil have been reported, where wettability plays an important role. The relative permeability correlations often fail to predict what is seen in the experiments.

7.6 History dependent relative permeability correlations for three-phase flow

In order to describe the experimental data correctly many mechanisms must be included in the model. It must be possible to use different relative permeabilities for gas depending on if the gas saturation is decreasing or increasing. It should be possible to use a different gas relative permeability for three-phase flow when compared to two-phase flow, that is gas relative permeability dependent on both gas

and water saturations. The gas modelling must include gas trapping, and the relative permeability should be able to vary with gas trapping history.

It should be possible to use different water relative permeability with increasing versus decreasing water saturation. The water relative permeability should be able to depend on gas saturation in addition to water saturation, i.e. different water relative permeability for three-phase flow when compared to two-phase flow.

The residual oil is often lower when trapped gas is present (see chapter 10). A three-phase relative permeability model for oil must take this into account. The oil relative permeability should be modelled with dependence on gas and water saturation, as in the earlier discussed models. The oil relative permeability should also be history dependent.

Three-phase correlations with hysteresis and trapped gas have been introduced to take the complex three-phase behaviour into account. Larsen and Skauge[72] have made a history dependent model for three-phase relative permeability, which have been included in the Eclipse 100 simulator.[26] The model takes into account the effect of trapped gas on the residual oil saturation. The oil relative permeability is therefore process dependent. It is also possible to use different water relative permeabilities for two- and three-phase flow. The model allows reduced gas mobility in the three-phase case with gas trapping described by Carlson's[42] two-phase hysteresis model.

Egermann et. al[73] suggested an analytical expression for the hysteresis behaviour. The model was included in a reservoir simulator. The simulations of WAG experiments were successful.

7.7 Three-phase relative permeability from network modelling

Network models can also be used to predict three-phase relative permeability curves.[74-83] These models incorporate the physical rules of flow and the fluid placement in the pores. These models can be used to simulate the processes taking

place inside the pores. See chapter 8 or the paper by Blunt[29] for more details on network modelling.

8. Three-phase modelling in a network model

Van Dijke et. al[84-89] have developed a process based model for three-phase behaviour. Pore geometry and wettability are input parameters to the network model.

The procedure for prediction of three-phase parameters is to first anchor the network model to the experimentally measured two-phase data. This determines the pore properties and wettability parameters in the network. The three-phase behaviour is then estimated by using this preconditioned network.[87-88]

8.1 Two-phase drainage in a network

Two-phase drainage can be illustrated by using a very simple pore size distribution, see figure 8.1. The frequency of the different pore sizes is evenly distributed between the maximum and minimum pore size.

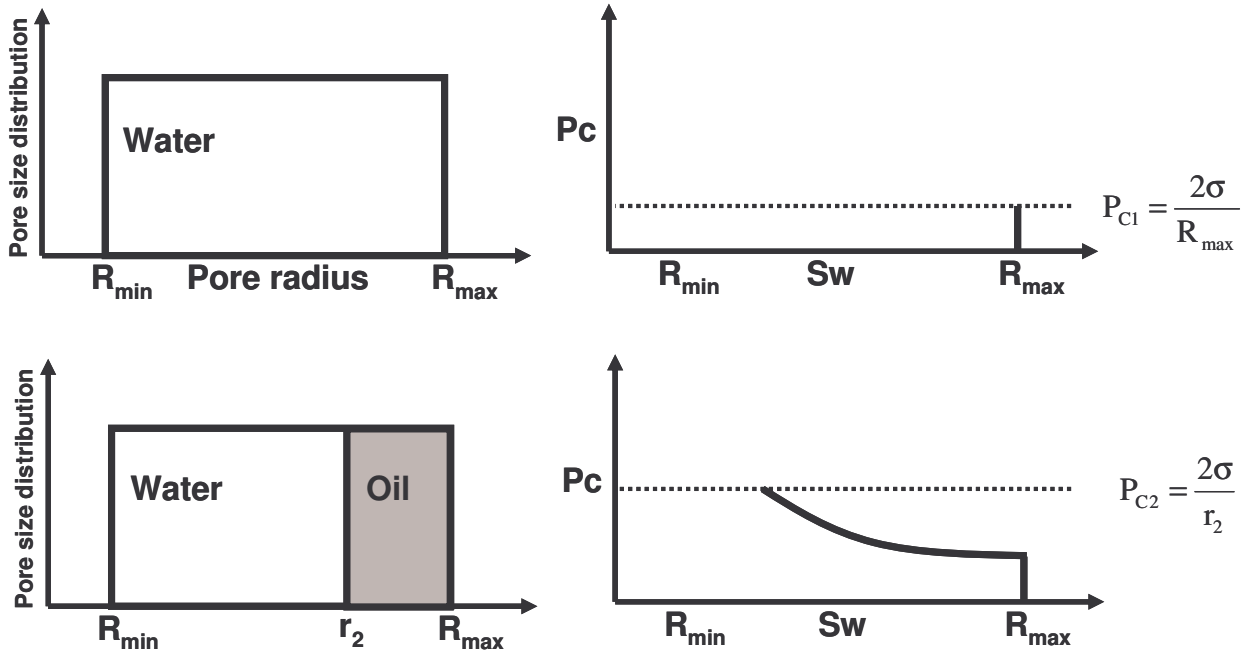

Figure 8.1: Primary drainage process (Adapted from Sorbie and van Dijke[85]).

The condition for entry of an invading fluid into a pore is that the pressure has reached a value, which is higher than the entry pressure of that pore,[84]

$$P_C > P_{C,entry} . \tag{49}$$

As seen in figure 8.1, the pressure has to reach the value

$$P_{C1} = \frac{2\sigma}{R_{\max}} \tag{50}$$

before the oil starts invading the largest pore with radius $R_{\max}$.

Accessibility is also an important parameter. Even though a pore satisfies the entry conditions, it cannot be invaded if the invading fluid is not yet connected to the pore. There can be pores with higher entry pressures standing in the way.

If the invading fluid has surrounded the initial fluid, the initial fluid can become trapped. In the case of a water-wet rock the initial fluid is water. If the water is trapped it has no connection to the outlet. It is however possible for the water to escape through films if the conditions for films are present in the system.

8.2 Two-phase imbibition in a network

Imbibition can happen by two different processes. The fluid can invade by piston-like displacement, see figure 8.2 a). The invading fluid pushes the initial fluid, out of the pore with a clearly defined front. The other process is invasion by snap-off, see figure 8.2 b). The invading fluid is then flowing along the walls of the pores and when the film of the invading fluid becomes thick enough it connects in the middle of the pore. In the case of a water-wet rock the invading fluid is water.

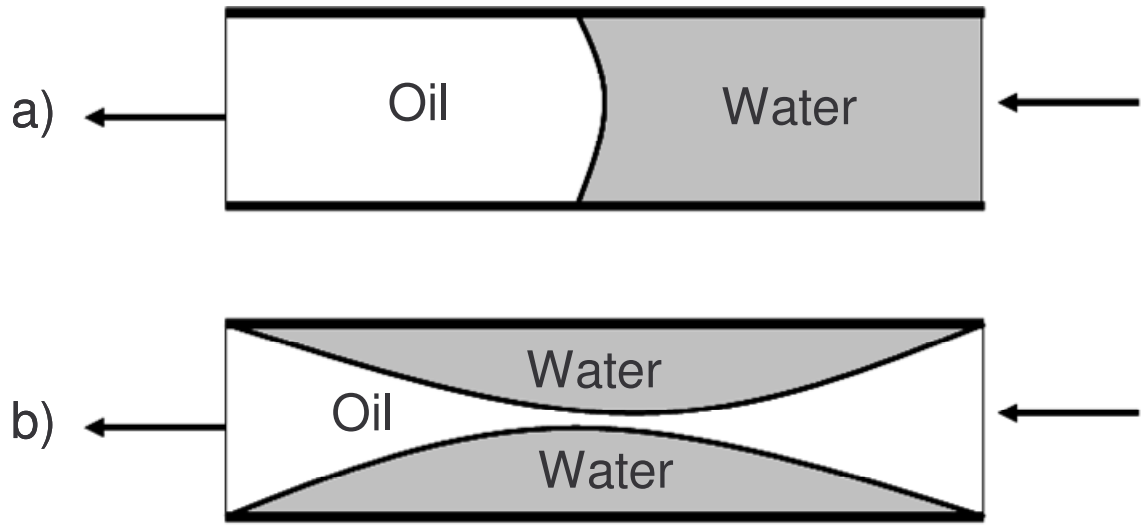

Figure 8.2: a) Piston like and b) snap-off displacement in the imbibition process.

The capillary pressure for snap-off is lower than the capillary pressure for piston-like displacement.[87] The capillary pressure for piston-like displacement is

$$P_C \propto \frac{2\sigma}{r}, \tag{51}$$

and the capillary pressure for snap-off for a strongly water-wet case is

$$P_C \propto \frac{\sigma}{r}. \tag{52}$$

Remember that capillary pressure is defined as

$$P_C = P_{non-wetting} - P_{wetting} \tag{53}$$

If the pressure of the non-wetting phase occupying the pore is lowered the capillary entry pressure for piston-like displacement is reached first. If the front of the wetting fluid has not reached the pore, piston-like displacement will not take place. Snap-off can still occur if there are films of the wetting fluid present in the pore. Snap-off will

then happen if the pressure of the non-wetting phase gets even lower, or the pressure of the wetting fluid is increased. In a fully accessible capillary bundle model only piston-like displacement will occur.

8.3 3D network model

A 3D network model for describing three-phase behaviour was constructed at Heriot-Watt[84-86]. A picture of the software which shows the network can be seen in figure 8.3.

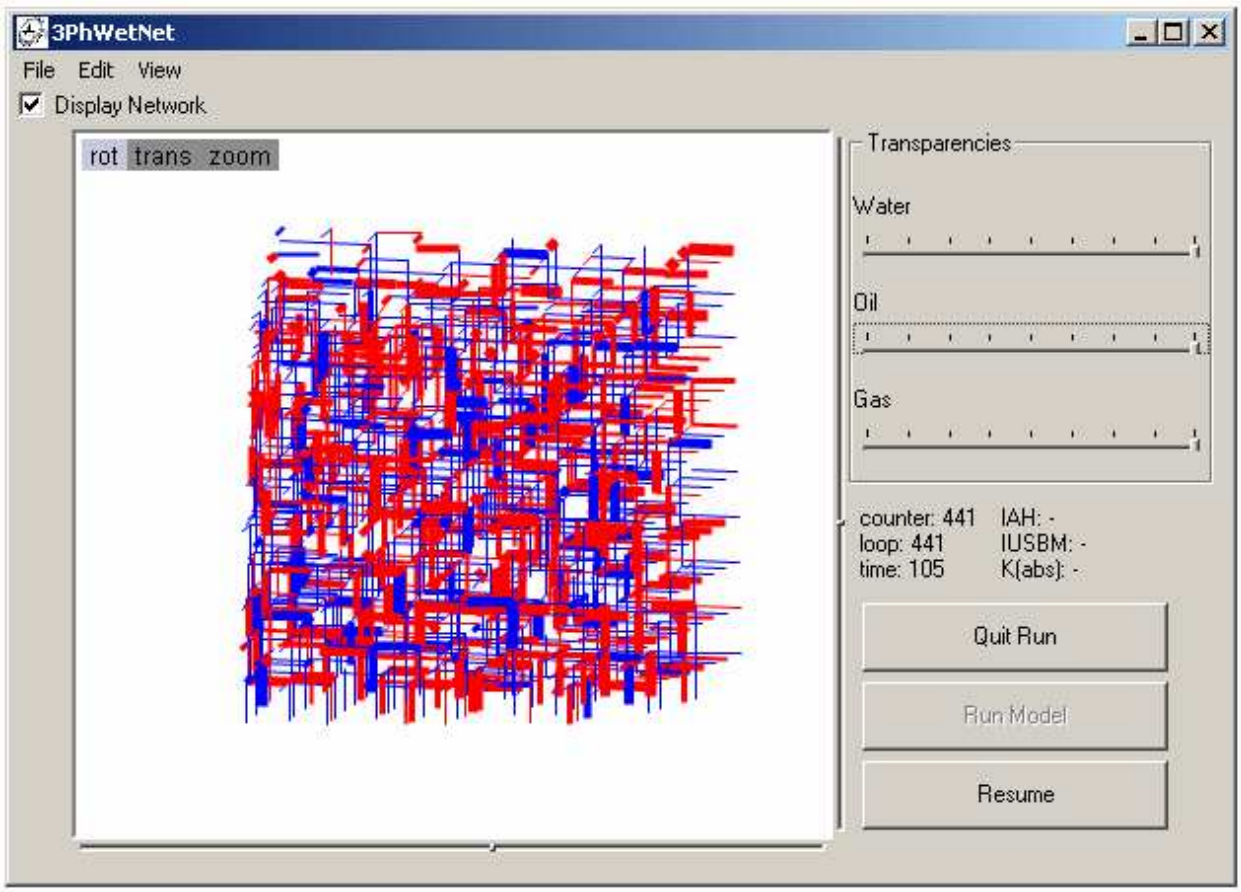

Figure 8.3: Network model.

The pore radius, r, can be used to quantify the capillary pressure, volume of the pore and the conductance of the pore. All three parameters are functions of the pore radius

$$P_C \propto \frac{1}{r}, \tag{54}$$

$$V \propto r^{\nu} \text{ and} \tag{55}$$

$$g \propto r^{\lambda}, \tag{56}$$

where V is the volume, ν is the volume exponent, g is the conductance and λ is the conductance exponent.

In order to describe the network several parameters are necessary

- Minimum and maximum pore size ($R_{\min}$ and $R_{\max}$),
- Pore size distribution (if exponential distribution, the exponent n must be specified),
- Volume exponent (ν , typically between 0 and 4),
- Conductivity exponent (g , typically between 2 and 4),
- Coordination number, how well the network is connected (z , typically between 2.5 and 6),
- Wettability (wettability type, $\cos\theta_{ow}$, fraction of oil-wet and water-wet pores etc.) and
- Existence of films and layers.

8.4 Contact angle relations for weakly wetted pores

The Bartell and Osterhof [7] equation states that

$$\sigma_{gw}\cos\theta_{gw} - \sigma_{go}\cos\theta_{go} - \sigma_{ow}\cos\theta_{ow} = 0. \tag{57}$$

For weakly wetted pores Sorbie and van Dijke[89] proposed the linear relationships for non-spreading oil

$$\cos\theta_{go} = \frac{1}{2}\left\{-1+\frac{\sigma_{gw}-\sigma_{ow}}{\sigma_{go}}\cos\theta_{ow}+1+\frac{\sigma_{gw}-\sigma_{ow}}{\sigma_{go}}\right\} \text{ and} \tag{58}$$

$$\cos\theta_{gw} = \frac{1}{2}\left\{1-\frac{\sigma_{go}-\sigma_{ow}}{\sigma_{gw}}\cos\theta_{ow}+1+\frac{\sigma_{go}-\sigma_{ow}}{\sigma_{gw}}\right\}. \tag{59}$$

Figure 8.4 illustrates the contact angle relationship.

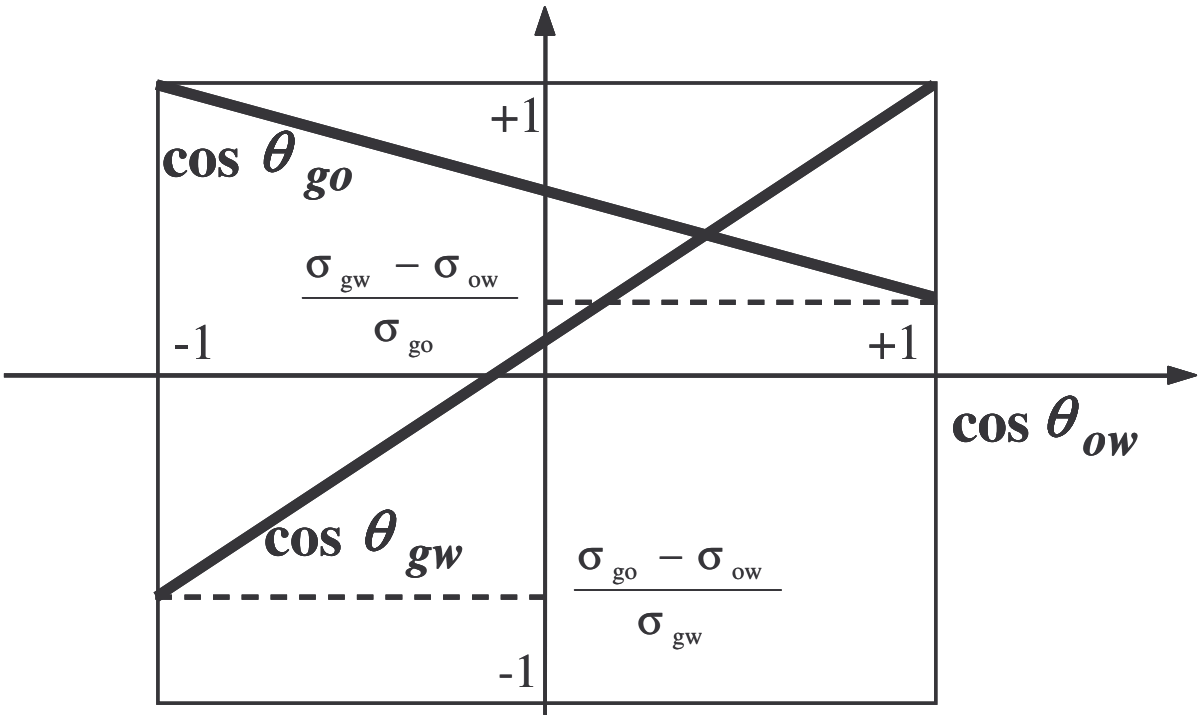

Figure 8.4: Contact angle relations for non-spreading oil (Adapted from Sorbie and van Dijke[89]).

For spreading oil they proposed

$$\cos\theta_{go} = 1 \text{ and} \tag{60}$$

$$\cos\theta_{gw} = \frac{\sigma_{ow}}{\sigma_{gw}}\cos\theta_{ow}+\frac{\sigma_{go}}{\sigma_{gw}} \tag{61}$$

Figure 8.5 shows the contact angle relationship for spreading oil.

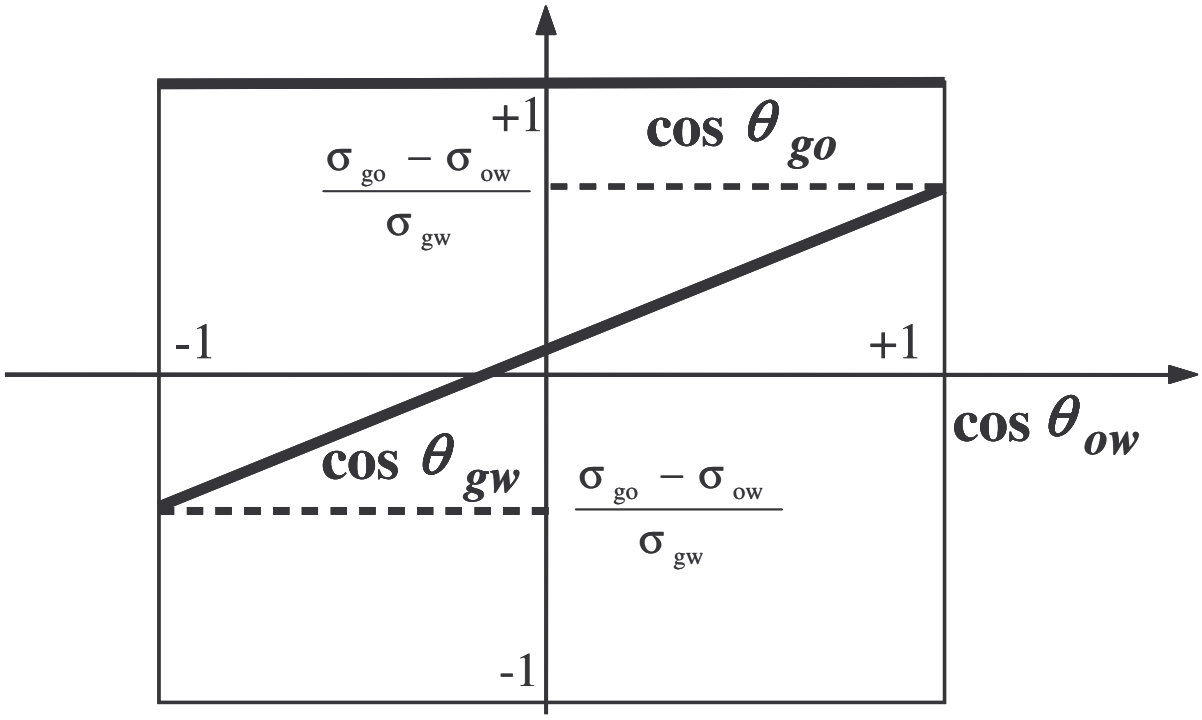

Figure 8.5: Contact angle relations for spreading oil (Adapted from Sorbie and van Dijke[89]).

This can be reformulated to a general expression for both spreading and non-spreading cases in terms of the spreading coefficient[89]

$$\cos\theta_{go} = \frac{1}{2\sigma_{go}}\left\{C_{S,o}\cos\theta_{ow} + C_{S,o} + 2\sigma_{go}\right\} \text{ and} \tag{62}$$

$$\cos\theta_{gw} = \frac{1}{2\sigma_{gw}}\left\{\left(C_{S,o} + 2\sigma_{ow}\right)\cos\theta_{ow} + C_{S,o} + 2\sigma_{go}\right\}, \tag{63}$$

where

$$C_{S,o} = \begin{cases} \sigma_{gw}\text{-}\sigma_{go}\text{-}\sigma_{ow} & \text{if} \quad \sigma_{gw}\text{-}\sigma_{go}\text{-}\sigma_{ow} < 0 \\ 0 & \text{if} \quad \sigma_{gw}\text{-}\sigma_{go}\text{-}\sigma_{ow} > 0 \end{cases}. \tag{64}$$

The wetting order of water, oil and gas can be determined for a pore with any value of $\cos\theta_{ow}$.

8.5 Pore filling sequence

The entry condition, eq. 50, will decide the pore filling sequence. The invasion will start in the pores with the smallest entry pressure.

One example of a pore filling sequence is shown in figures 8.6 to 8.9. Water is invading oil-filled pores. Figure 8.6 illustrates a mixed-wet porous medium with large pores oil-wet and small pores water-wet. The pores are initially filled with oil.

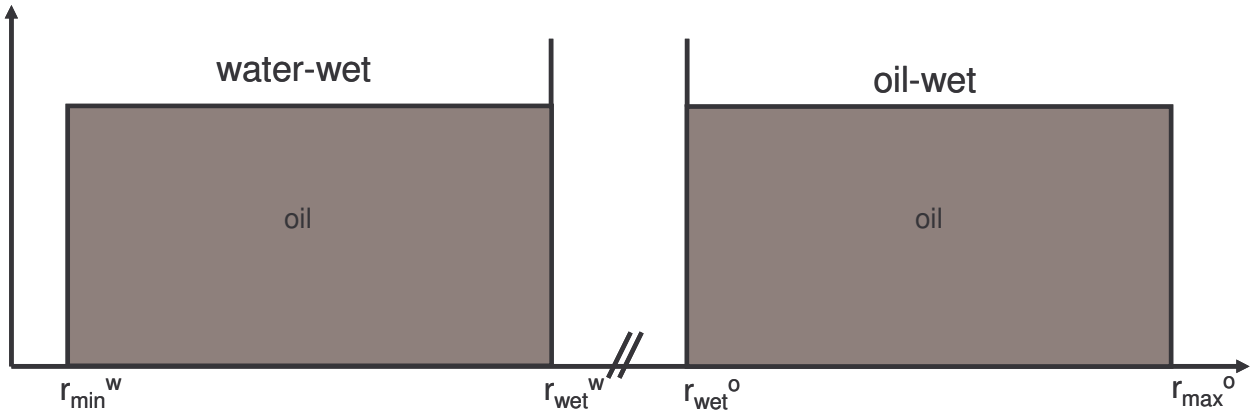

Figure 8.6: Mixed-wet medium with oil filled pores (Adapted from Sorbie and van Dijke[89]).

Water is invading the pores starting from the smallest pores because these pores have the lowest entry pressure, see figure 8.7,

$$P_{entry,w}(r_{\min}{}^{w}) = P_o - \frac{2\sigma_{ow}}{r_{\min}{}^{w}} \quad . \tag{65}$$

The ordering of the capillary entry pressures can be found from

$$\frac{2\sigma_{ow}}{r_{\min}^{w}} > \frac{2\sigma_{ow}}{r_{wet}^{w}} > -\frac{2\sigma_{ow}}{r_{\max}^{o}} > -\frac{2\sigma_{ow}}{r_{wet}^{o}}. \qquad (66)$$

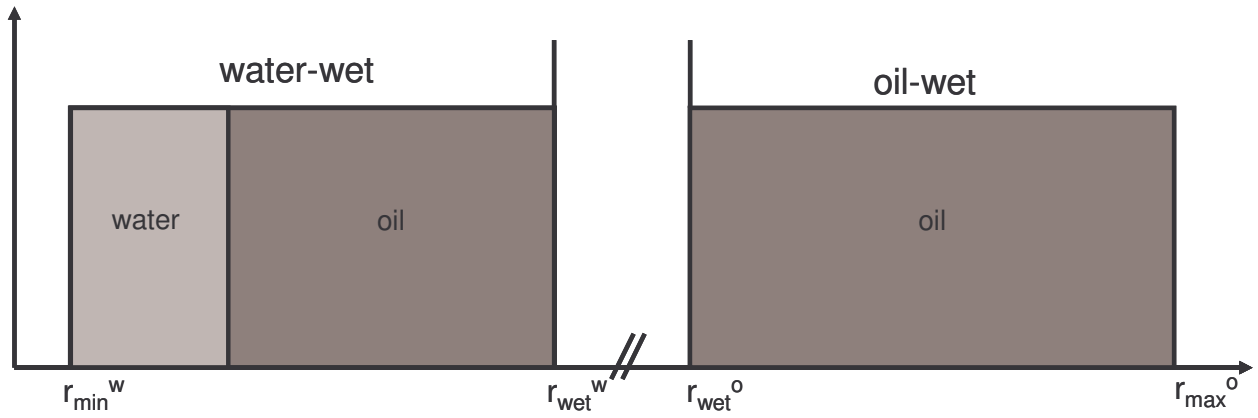

Figure 8.7: Water is invading starting with the smallest water-wet pores (Adapted from Sorbie and van Dijke[89]).

All the water-wet pores are filled first because the entry pressures for all the water-wet pores are lower than any entry pressure in the oil-wet pores, see figure 8.8.

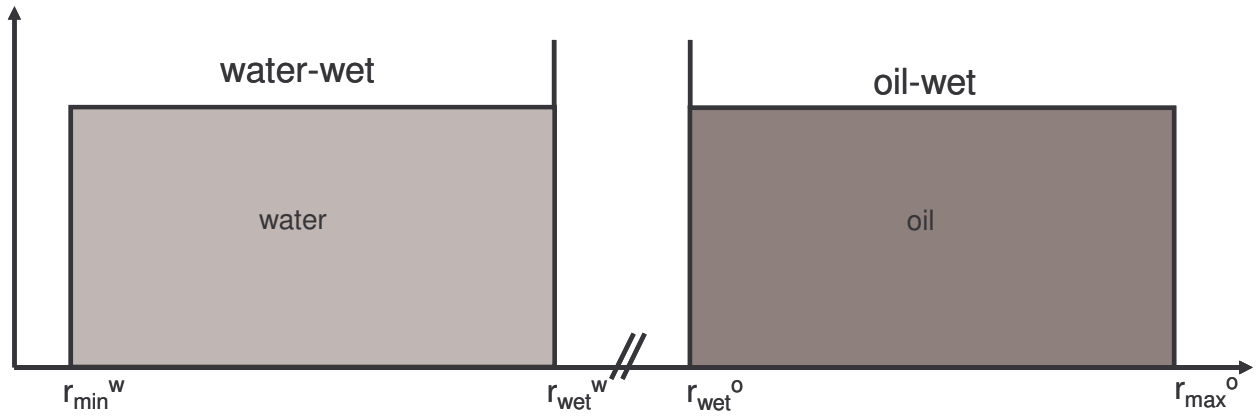

Figure 8.8: All the water-wet pores have been invaded (Adapted from Sorbie and van Dijke[89]).

After all the water-pores are invaded the water starts invading from the largest oil-wet pores, see figure 8.9. The largest oil-wet pore has a lower entry pressure than the smallest oil-wet pore, seen from eq. 67.

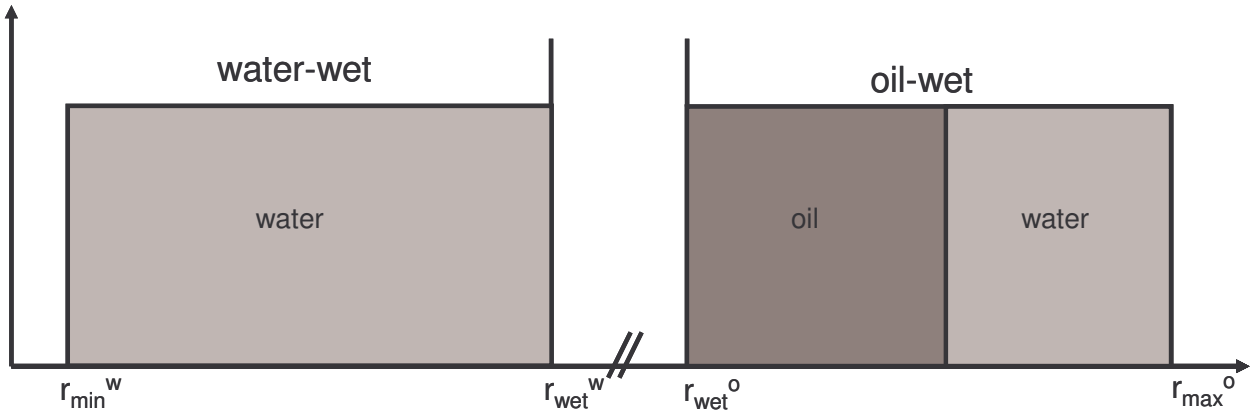

Figure 8.9: Water is invading oil filled pores (Adapted from Sorbie and van Dijke[89]).

8.6 Pore occupancy for three phases

The pore filling can result in a number of pore occupancies. Three types of occupancies can occur. When oil is intermediate wet, oil has boundaries with both water and gas, we have a type I occupancy. Type II occupancy occurs if gas is intermediate wet and type III if water is intermediate wet.[84]

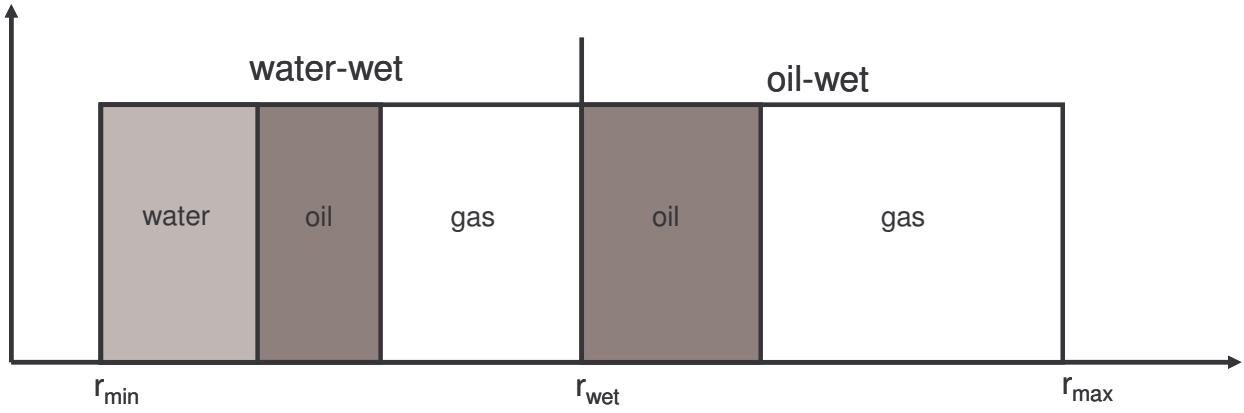

Figure 8.10: Type I; oil is intermediate wetting (Adapted from Sorbie and van Dijke[89]).

In the type I case, see figure 8.10, the gas-water capillary pressure and the relative permeability of oil are functions of two saturations[84]

$$P_{Cgw}(S_w, S_g) = P_{Cgo}^{2-phase}(1-S_g) + P_{Cow}^{2-phase}(S_w) \text{ and} \tag{67}$$

$$k_{ro}(S_w, S_g) = 1 - k_{rg}^{2-phase,go}(S_g) - k_{rw}^{2-phase,ow}(S_w)\,. \tag{68}$$

The other capillary pressures and relative permeabilities are functions of one saturation value[84]

$$P_{Cgo}(S_g) = P_{Cgo}^{2-phase}(1-S_g)\,, \tag{69}$$

$$P_{Cow}(S_w) = P_{Cow}^{2-phase}(S_w)\,, \tag{70}$$

$$k_{rg}(S_g) = k_{rg}^{2-phase,go}(S_g) \text{ and} \tag{71}$$

$$k_{rw}(S_w) = k_{rw}^{2-phase,ow}(S_w)\,. \tag{72}$$

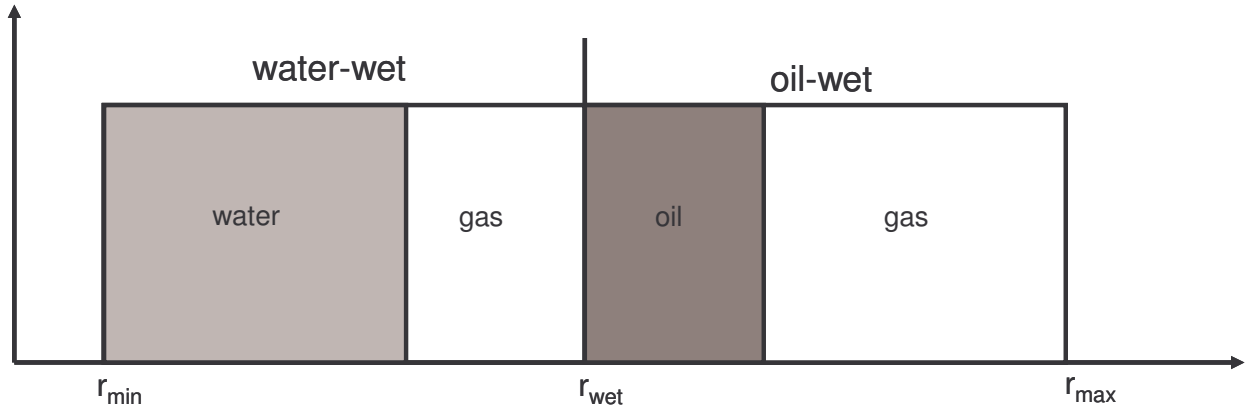

Figure 8.11: Type II; gas is intermediate wetting (Adapted from Sorbie and van Dijke[89]).

For type II, see figure 8.11, gas is intermediate wetting i.e. has boundaries with both water and oil. The oil-water capillary pressure and the relative permeability of gas are functions of two saturations[84]

$$P_{Cow}(S_w, S_o) = P_{Cgw}^{2-phase}(S_w) - P_{Cgo}^{2-phase}(S_o) \text{ and} \tag{73}$$

$$k_{rg}(S_w, S_o) = 1 - k_{rw}^{2-phase,gw}(S_w) - k_{ro}^{2-phase,go}(S_o). \tag{74}$$

The rest of the capillary pressures and relative permeabilities are functions of one saturation value[84]

$$P_{Cgo}(S_o) = P_{Cgo}^{2-phase}(S_o), \tag{75}$$

$$P_{Cgw}(S_w) = P_{Cgw}^{2-phase}(S_w), \tag{76}$$

$$k_{ro}(S_o) = k_{ro}^{2-phase,go}(S_o) \text{ and} \tag{77}$$

$$k_{rw}(S_w) = k_{rw}^{2-phase,gw}(S_w). \tag{78}$$

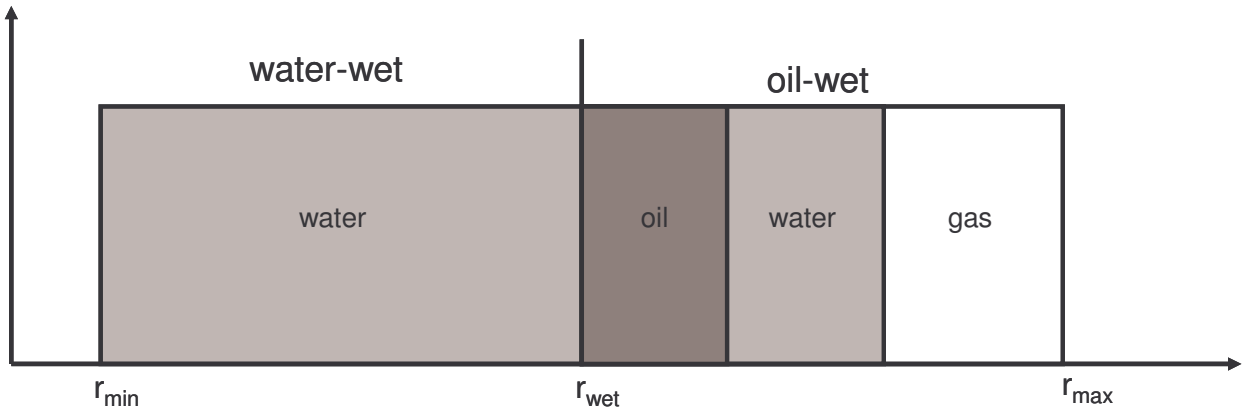

Figure 8.12: Type III; water is intermediate wetting (Adapted from Sorbie and van Dijke[89]).

In the type III case, see figure 8.12, the water is intermediate wetting and the gas-oil capillary pressure and the relative permeability of water are functions of two saturations[84]

$$P_{Cgo}(S_g, S_o) = P_{Cgw}^{2-phase}(1-S_g) - P_{Cow}^{2-phase}(1-S_o) \text{ and} \tag{79}$$

$$k_{rw}(S_o, S_g) = 1 - k_{ro}^{2-phase,ow}(S_o) - k_{rg}^{2-phase,gw}(S_g). \tag{80}$$

The rest of the capillary pressures and relative permeabilities are functions of one saturation value[84]

$$P_{Cow}(S_o) = P_{Cow}^{2-phase}(1-S_o), \tag{81}$$

$$P_{Cgw}(S_g) = P_{Cgw}^{2-phase}(1-S_g), \tag{82}$$

$$k_{ro}(S_o) = k_{ro}^{2-phase,ow}(S_o) \text{ and} \tag{83}$$

$$k_{rg}(S_g) = k_{rg}^{2-phase,gw}(S_g). \tag{84}$$

9. Three-phase modelling in Eclipse 100

9.1 Modelling of lower residual oil for three-phase

The residual oil saturation is usually lower for three-phase flow than for two-phase flow. The SOMWAT-keyword[90] specifies the minimum oil saturation as a function of water saturation, see figure 9.1. The first column is the water saturation and the second column is the residual oil saturation. The first row lists the minimum water saturation and the residual oil after two-phase gas injection, and the last row lists the maximum water saturation and the residual oil after two-phase water injection. This is a static change of the minimum residual oil saturation, S_{orm}.

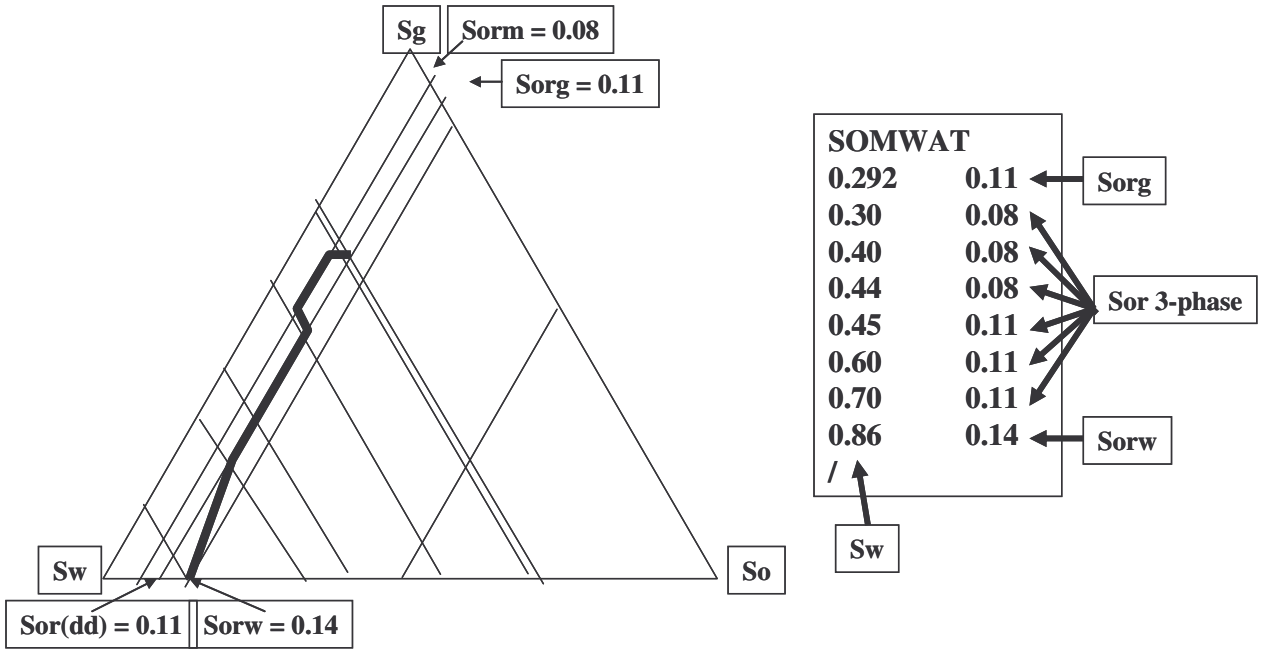

Figure 9.1: SOMWAT; Minimum oil saturation as a function of water saturation.

Trapping of gas can lead to lower minimum oil saturation. This is often described by the equation

$$S_{orm} = S_{orw} - R \cdot S_{gt}, \tag{85}$$

where S_{orm} is the minimum residual oil saturation, S_{orw} is the residual oil after water injection, R is a constant between 0 and 1 and S_{gt} is the trapped gas saturation.

The amount of gas trapped is often described by the Land constant, see equation 41. The effect of gas trapping can be modelled using the WAGHYSTR-keyword[90], see figure 9.2. The first number is the Land constant, the third item is the flag for the modification of residual oil by trapped gas and the last parameter is the fraction of the trapped gas which is modifying residual oil (the R-constant in equation 85). This is a dynamic change of S_{orm}.

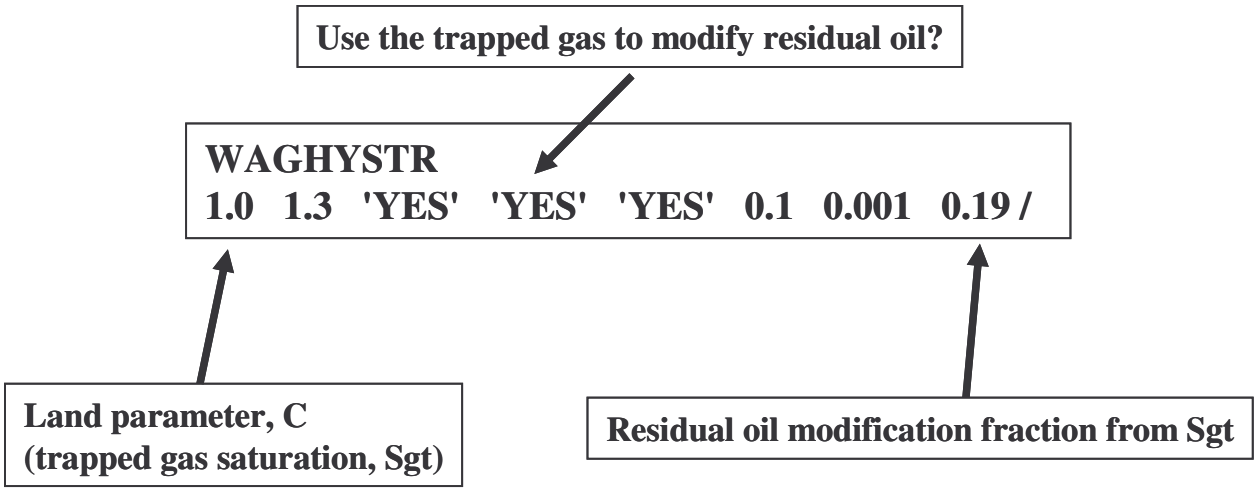

Figure 9.2: WAGHYSTR; trapped gas is modifying residual oil.

9.2 Modelling of double displacement

When gas is injected into an oil and water filled core the gas can displace oil directly, but a double displacement could also occur. Double displacement takes place when the gas displaces oil, which again displaces water. This leads to less oil production and more water production when compared to direct displacement. Figure 9.3 shows an illustration of direct displacement on top and double displacement below.

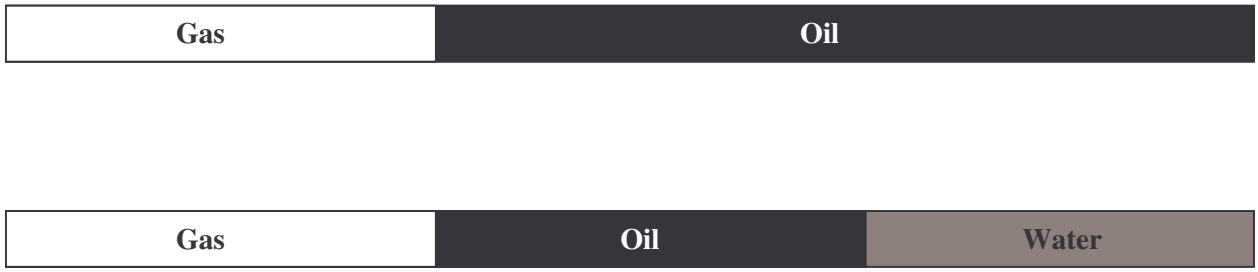

Figure 9.3: Direct displacement and double displacement.

Double displacement is more likely to occur at the beginning of the gas injection period, when the water saturation is high. At the end of the gas injection period the water saturation is low and direct displacement will dominate. This can lead to lower residual oil at the end of the gas injection when compared to the early period of gas injection. This behaviour can be modelled by the SOMWAT-keyword[90]. The double displacement, at high water saturation, has higher residual oil saturation, as seen in figure 9.4.

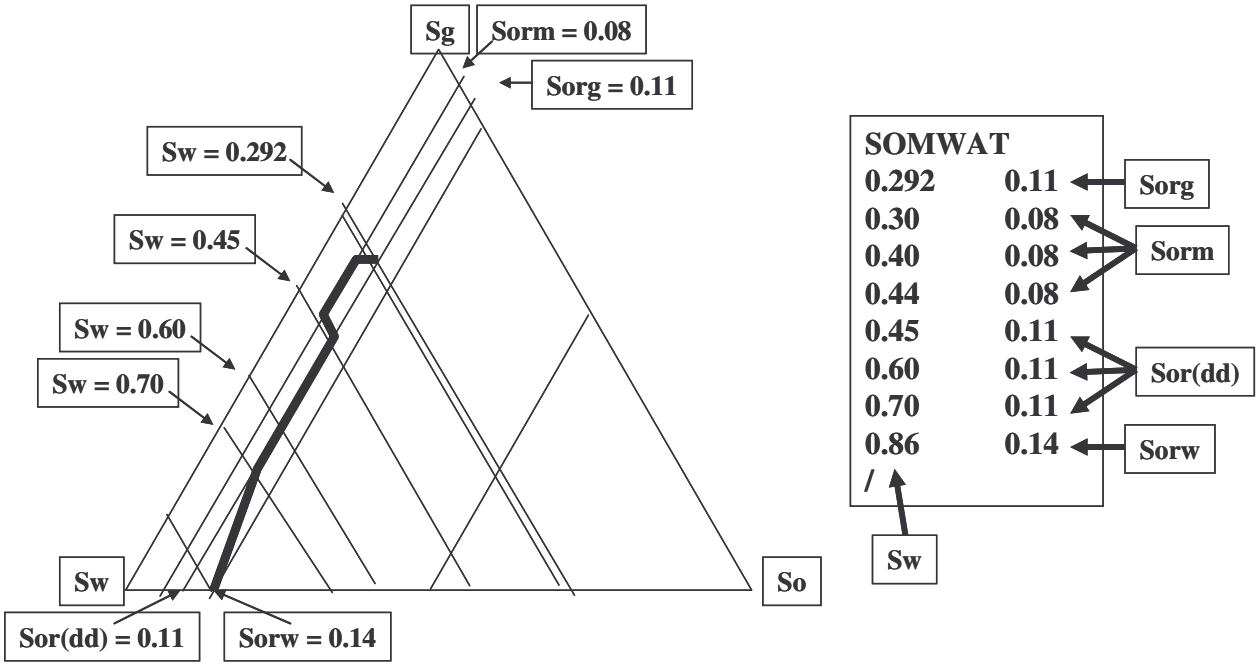

Figure 9.4: Double displacement period (Sw ≥ 0.45) has higher residual oil saturation, Sor(dd)= 0.11, than the residual oil at the end of the G2 injection Sorm = 0.08.

9.3 Modelling of hysteresis and three-phase relative permeability

Three-phase relative permeability is difficult to measure experimentally. Different models are used to estimate three-phase relative permeability from two-phase relative permeability. One example is the Stone I correlation. The relative permeability of oil is a function of the three saturation values, S_o, S_w and S_g, the two-phase relative permeability of oil in presence of water, k_{row}, and in presence of gas, k_{rog}.

Hysteresis refers to the fact that relative permeability is directional dependent; it has different values for a saturation value depending on whether the saturation is increasing or decreasing.

The three-phase relative permeability of oil is modelled by requesting the Stone I model using the STONE1-keyword[90]. Other three-phase models are also available and have been compared by Kossack[91].

The WAGHYSTR-keyword[90] can be used to model hysteresis see figure 9.5. The second value is the factor for reduction of gas mobility in three-phase flow, the third entry is the flag for use of the WAG Hysteresis model for the gas relative permeability, entry four is the flag for use of trapped gas saturation to modify the residual oil used in Stone I, and the fifth item is the flag for use of the WAG Hysteresis model for the water phase.

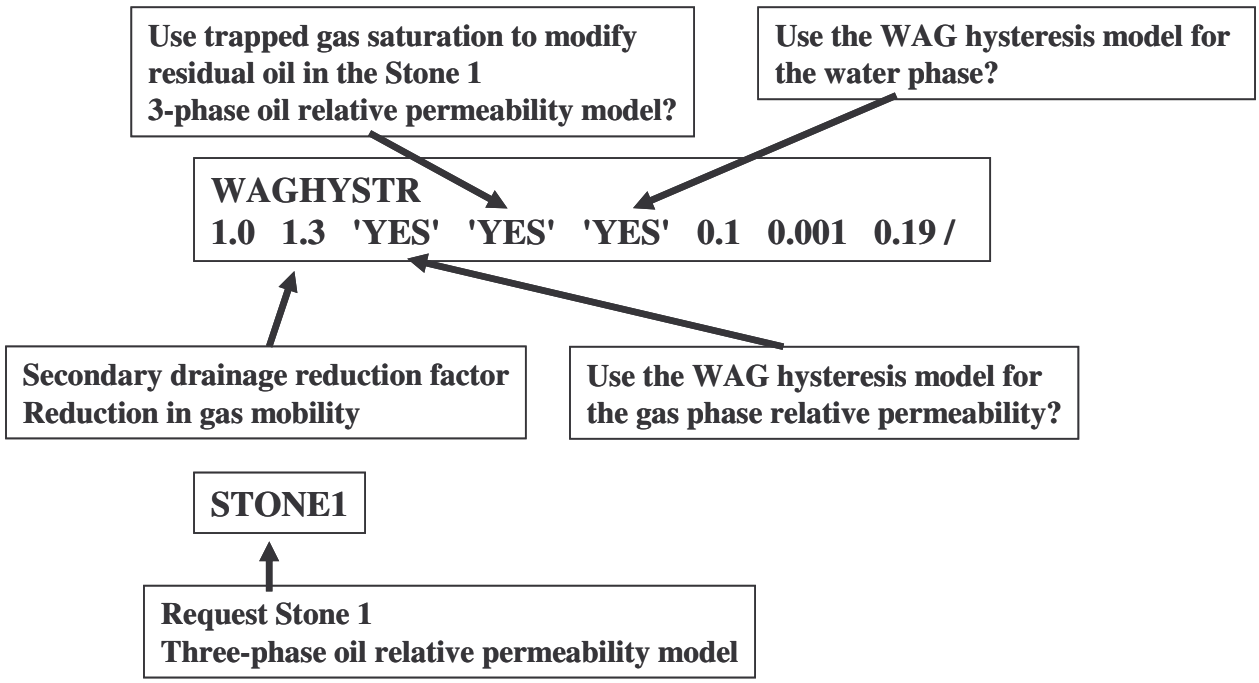

Figure 9.5: STONE1 and WAGHYSTR; modelling of hysteresis and three-phase relative permeability.

10. Summary of main results

10.1 Three-phase features

The parameters governing three-phase flow and the relationship between these parameters have been described in several papers. A summary of the most important findings will be presented here.

It has been observed that the three-phase residual oil saturation is lower than after two-phase flow. This has been linked to the trapped gas saturation. Trapped gas will often result in lower residual oil. The effect that the trapped gas saturation has on residual oil has been connected to wettability. The amount of trapped gas has been associated with wettability, process and initial or maximum gas saturation.[92-104]

The wetting phase has generally shown little hysteresis in relative permeability. For strongly water-wet cases the relative permeability of water has often been found to be a function of its own saturation. The relative permeability of oil in oil-wet cores is usually a function of its own saturation.[40,92-96] The intermediate-wetting phase has shown some hysteresis in most cases. Water-wet cores show three-phase hysteresis for oil relative permeability, and oil-wet cores show hysteresis for the water relative permeability.[92-93,95-96] The gas is usually the non-wetting phase, and the gas relative permeability generally shows strong hysteresis for all wettabilities.[40,93-95] In neutrally-wet cases the behaviour is complex. In a mixed-wet case all the phases showed hysteresis in the relative permeability.[95]

In this work a large number of three-phase core flooding experiments were collected in a database and analysed. The three-phase effects and connections between different parameters were investigated. The results are presented in paper 1.

The three-phase residual oil saturation was significantly lower than the residual oil after only gas injection or only water injection. In a water-wet core the residual oil saturation appears to be lower when gas is injected first in a WAG-sequence, and for

an oil-wet core the residual oil seems to be lower when water is injected first in a WAG-sequence. In the case of initial gas injection the residual oil becomes lower for more oil-wet cores than for water-wet cores.

Trapped gas leads to lower residual oil. The effect is usually quantified by the R-factor in the equation

$$S_{orm} = S_{orw} - R \times S_{gt}\,, \tag{86}$$

where S_{orm} is the minimum residual oil saturation, S_{orw} is the residual oil after water injection and S_{gt} is the trapped gas saturation.

The effect of trapped gas on residual oil was strongest in water-wet cores when compared to more oil-wet cores. The impact of trapped gas was higher for WAG-flooding than for tertiary water injection (after initial water injection and secondary gas injection), which had a higher impact of trapped gas than secondary water injection (after initial gas injection).

There was a strong connection between the initial or maximum gas saturation and the trapped gas saturation. This can be quantified by the Land constant[40]

$$C = \frac{1}{S_{gt}} - \frac{1}{S_{gi}}\,, \tag{87}$$

where S_{gi} is the initial or maximum gas saturation

The average trapped gas saturation was higher for secondary water injection after gas injection than for WAG-injection, which has short slugs of gas and water.

Hysteresis in relative permeability was also studied. In general significant hysteresis effects are found for the gas relative permeability in almost all cases. Hysteresis was found for the water relative permeability in some cases.

Multivariate analysis showed that the three-phase residual oil saturation was correlated with the residual oil after water injection and negatively correlated with the trapped gas saturation, in agreement with equation 86.

The trapped gas saturation was related to the initial gas saturation, in agreement with equation 87. Trapped gas was also correlated with absolute permeability and the endpoint water relative permeability.

10.2 The effect of capillary pressure in history matching

One of the important parameters influencing three-phase flow is capillary pressure. Relative permeability has usually been calculated by analytical methods[105-107], where the effect of capillary pressure has been neglected. More resent inverse methods[108-109] have included capillary pressure in the estimation of relative permeability. The inverse method was used in this work.

The effect of capillary pressure on two- and three-phase flow was studied by use of a simulation model, Eclipse 100. The results are discussed in paper 2 and in more detail in paper 3. A history match of a core flooding experiment with and without capillary pressure was performed. Two-phase, gas-oil and oil-water, capillary pressure curves were used as input. The capillary pressure had a significant effect on the shape of the oil production curve, the total oil recovery and the differential pressure for both two- and three-phase flow.

A history match without capillary pressure was first done by tuning the relative permeability curves. Then capillary pressure was included and the result was that the total oil recovery was much lower. The capillary pressure clearly had a large effect on the flow. This was seen for both initial gas injection and initial water injection, and also for three-phase flow.

In order to get a new match with capillary pressure the relative permeability curves had to be changed. The relative permeability of oil had to be increased and the relative permeability of the injected fluids had to be decreased.

The new history match with capillary pressure was closer to the experimental data than the match without capillary pressure. The shape of the total oil production curve and the differential pressure was better matched with the experimental data.

Three-phase flow was modelled both with the two-phase capillary pressure and with Killough's model[23] for three-phase capillary pressure. The match of the experimental data was better when two-phase capillary pressure was used for three-phase flow, than when using Killough's correlation[23].

10.3 Impact of three-phase characteristics and capillary pressure

The size of the three-phase area has a large effect on the total oil recovery, because the three-phase zone has lower residual oil.[93,100] The analytical methods for estimating the three-phase zone may strongly underestimate the size. [110-111] Simulation studies have shown larger three-phase zones.[112-116]

It has been shown that the three-phase relative permeability is significantly different from the two-phase relative permeability. The relative permeabilities of the injected fluids, gas and water, is reduced in the three-phase zone.[67]

The effect of three-phase features and capillary pressure on field scale was investigated. The effect on the size of the three-phase zone, breakthrough time of the injected fluids and oil recovery was studied by using a black oil simulator. The results are presented in paper 4.

In three-phase flow the relative permeability of the injected fluids are lower and this delays the segregation of gas and water. The three-phase zone is therefore bigger when these effects are taken into account. Another important three-phase effect is gas trapping. Gas trapping often leads to lower residual oil. Using three-phase

representations of relative permeability and including gas trapping effects gave a larger three-phase zone, later breakthrough of injected fluids and higher oil recovery.

In paper 2 and 3 it was found that the capillary pressure had a significant effect on history matching of a core flooding experiment. It was therefore important to find out how capillary pressure influenced the flow on field scale. The work described in paper 3 indicated that using two-phase capillary pressure for three-phase flow gave better results than using Killough's three-phase capillary pressure correlation. Two-phase capillary pressure curves were therefore used in the field scale study.

The results showed that capillary pressure also had a significant effect on field scale. Including capillary pressure delayed the segregation of gas and water even more than when capillary pressure was neglected. In paper 3 it was found that the relative permeability of the injected fluids is lower when capillary pressure is included. Inclusion of this effect further delayed the segregation of gas and water. The three-phase zone was even bigger and the oil recovery was higher.

10.4 Three-phase capillary pressure

Two-phase capillary pressure is often measured experimentally and can be included in reservoir simulations. Three-phase capillary pressure is very difficult to measure, and methods for estimation of three-phase capillary pressure must be used.

When studying the effect of capillary pressure on three-phase flow it is important to model the three-phase capillary pressure correctly. In simulations the two-phase capillary pressure is often used also for three-phase flow, or Killough's model[23] can be used to describe the three-phase capillary pressure. Paper 3 indicated that using two-phase capillary pressure gives better results than using Killough's correlation. A network model was used to try and predict the three-phase capillary pressure and compare it with the two-phase capillary pressure and Killough's model.

The concept of using a network of pores to model flow in porous media was first described by Fatt[117-119] in 1956. The concept was not further investigated before the

1980s, when percolation theory was incorporated in network models.[120-122] The network models can be used to explain and predict many pore scale phenomena. Network models have been used to predict parameters like three-phase relative permeabilities and three-phase capillary pressures.[29-33,74-83,87-88]

In this work a network model developed at the Heriot-Watt University[84-89] was used to investigate three-phase capillary pressure. The work is discussed briefly in paper 2 and in more detail in paper 5. The network model was anchored to the experimentally measured two-phase, gas-oil and oil-water, capillary pressure curves. The pore geometry and wettability was established in the anchoring process. This was done partly by trial and error. A more automatic method for matching the two-phase data using an ensemble Kalman filter is demonstrated in paper 6.

After anchoring the network model to the two-phase data, the three-phase capillary pressure was predicted using the same geometry and wettability. The three-phase gas-oil capillary pressure had a higher positive value than for two-phase, and the three-phase oil-water capillary pressure had a higher negative value than for two-phase. The three-phase capillary pressure loop was outside the two-phase capillary pressure loop.

Killough's model[23] assumed that the three-phase gas-oil and oil-water capillary pressure was a weighted average of the two-phase curves. In this model the three-phase capillary pressure curves were inside the two-phase capillary pressure loop. The conclusion was therefore that Killough's model could not be used to describe the three-phase capillary pressure predicted by the network model.

Paper 7 gives a summary of important progress in modelling of immiscible WAG. The main issues discussed are relative permeability hysteresis and capillary pressure. The results from this work are discussed together with earlier work in this research area.

11. Further work

In paper 6 a method for generating three-phase capillary pressure surfaces from a network model anchored to measured two-phase data is described. The three-phase data is defined for all saturation values. Tables are written from the three-phase capillary pressure surfaces. These tables can be included in a reservoir simulator.

Eclipse 100 has an option for including two-dimensional tables for capillary pressure, but the tables are too restricted for our case. The capillary pressure values in Eclipse have to be lower for three-phase than for two-phase. This is not the case for the three-phase capillary pressure generated by the network model.

Other simulators have been considered for simulation with two-dimensional tables for the capillary pressure, but several problems occurred when trying to implement the tables. An in-house simulator, Athena, has been used with some success. The early results show slower segregation and thus a larger three-phase zone, when three-phase capillary pressure tables are included when compared to using two-phase capillary pressure.

References

1. Anderson, W. G.: ”Wettability Literature Survey – Part 4: Effects of Wettability on Capillary Pressure”, Journal of Petroleum Technology, Oct. 1987.
2. Bear, J.: “Dynamics of Fluids in Porous Media”, American Elsevier Publ. Co., New York, 1972.
3. Dake, L. P.: “Fundamentals of reservoir engineering”, Elsevier, 1997.
4. Mayer-Gürr, A.: “Petroleum engineering”, Ferdinand Enke Publishers, Stuttgart, 1976.
5. Zolotukhin, A. and Ursin, J. R.: ” Introduction to petroleum reservoir engineering”, Høyskoleforlaget, Kristiansand, 2000.
6. Ahmed, T.: “Reservoir Engineering Handbook”, Third Edition, Elsevier Inc., 2006.
7. Bartell, F. E. and Osterhof, H. J.: ”Determination of the Wettability of a Solid by a Liquid”, Ind. Eng. Chem., 19 (11), pp. 1277-1280, 1927.
8. Archer, J. S. and Wall, C. G.: “Petroleum Engineering: Principles and Practice”, Graham & Trotman, London, 1986.
9. Young, T.: “An Essay on the Cohesion of Fluids”, Philosophical Transactions of the Royal Society of London, 95, pp. 65-87, 1805.
10. De Laplace, P. S.: “Mechanique Celeste”, supplement to book 10, 1806.
11. Selley, R. C.: ”Elements of Petroleum Geology”, Academic Press, 1998.
12. Killins, C. R., Nielsen, R. F. and Calhoun, J. C.: “Capillary Desaturation and Imbibition in Porous Rocks”, Producers Monthly 18, No. 2, pp. 30-39, Dec. 1953.
13. Brooks, R. H. and Corey, A. T.: ”Hydraulic Properties of Porous Media”, Hydraulic Paper Number 3, Colorado State University, March 1964.
14. Standing, M. B.: “Notes on Relative Permeability Relationships”, unpublished report, Division of Petroleum Engineering and Applied Geophysics, The Norwegian Institute of Technology, The University of Trondheim, Aug. 1974.

15. Skjæveland, S. M., Siqveland, L. M., Kjosavik, A., Hammervold Thomas, W. L. and Virnovsky, G. A.: “Capillary Pressure Correlation for Mixed-Wet Reservoirs”, SPE Reservoir Evaluation & Engineering 3, pp. 60-67, Feb. 2000.
16. Thomeer, J. H. M.: ”Introduction of a Pore Geometrical Factor Defined by the Capillary Pressure Curve”, Journal of Petroleum Technology, pp. 73-77, Mars 1960.
17. Ma, S., Jiang, M. and Morrow, N. R.: “Correlation of Capillary Pressure Relationships and Calculations of Permeability”, SPE 22685, presented at the 66. Annual Technical Conference and Exhibition of the Society of Petroleum Engineers, Dallas, Texas, Oktober 6-9, 1991.
18. van Genuchten, M. T.: “A Closed-form Equation for Predicting the Hydraulic Conductivity of Unsaturated Soils”, Soil. Sci. Soc. Am. J. 44, pp. 892-898, 1980.
19. Lenhard, R. J. and Oostrom, M.: “A Parametric Model for Predicting Relative Permeability – Saturation – Capillary pressure Relationship of Oil – Water Sysytems in Porous Media with Mixed Wettability”, Transport in Porous Media, 31, pp. 109-131, 1998.
20. Delshad, M., Lenhard, R. J., Oostrom, M., Pope, G. A. and Yang, S.: “A Mixed-Wet Hysteretic Relative Permeability and Capillary Pressure Model in a Chemical Compositional Reservoir Simulator”, SPE 51891, presented at the SPE Reservoir Simulation Symposium, Houston, Texas, February 14-17, 1999.
21. Bentsen, R. G. and Anli, J.: “A New Displacement Capillary Pressure Model”, J. Cdn. Pet. Tech., pp. 75-79, 1976.
22. Huang, D. D., Honarpour, R. and Al-Hussainy, R.: “An Improved Model for Relative Permeability and Capillary Pressure Incorporating Wettability”, SCA 9718, presented at the SCA International Symposium, Calgary, Canada, September 7-10, 1997.
23. Killough, J. E.: “Reservoir Simulation with History-dependent Saturation Functions”, Trans. AIME 261, pp. 37-48, 1976.

24. Kleppe, J., Delaplace, P., Lenormand, R., Hamon, G. and Chaput, E.: “Representation of Capillary Pressure Hysteresis in Reservoir Simulation”, SPE 38899, 1997.
25. Helland J. O. Skjæveland S. M.: ”Three-phase Capillary Pressure Correlation for Mixed-wet Reservoirs,” SPE 92057. In: Proc SPE international petroleum conference in Mexico, Puebla, Mexico, November 2004.
26. Eclipse simulation software manual 2006.1, Technical description, Schlumberger.
27. Kalaydjian, F.J-M.: ”Performance and Analysis of Three-Phase Capillary Pressure Curves for Drainage and Imbibition in Porous Media” SPE 24878, 1992.
28. Virnovsky, G. O., Vatne, K. O., Iversen, J. E. and Signy, C.: ”Three-Phase Capillary Pressure Measurements in Centrifuge at Reservoir Conditions”, SCA2004-19, paper for the International Symposium of the Society of Core Analysts, Abu Dhabi, 5-9 October, 2004.
29. Blunt, M. J.: “Flow in porous media—pore-network models and multiphase flow”, Curr. Opin. Colloid Interface Sci, 6, pp. 197–207, 2001.
30. Mani, V. and Mohanty, K.K.: ”Pore-Level Network Modeling of Three-Phase Capillary Pressure and Relative Permeability Curves,” SPE Journal, September 1998, 238-248.
31. Fenwick, D. H. and Blunt, M. J.: “Network modelling of three-phase flow in porous media”, SPEJ 3(1), pp 86-97, 1998.
32. van Dijke, M. I. J., McDougall, S. R. and Sorbie, K. S.: ”Three-phase capillary pressure and relative permeability relationships in mixed-wet systems,” Trans. in Porous Media 44, pp. 1–32, 2001.
33. Suicmez, V. S., Piri, M. and Blunt, M. J.: “Pore-scale Simulation of Water Alternate Gas Injection”, Transport in Porous Media Vol. 66, No. 3, pp. 259-286, February 2007.
34. Adamson, A. W.: “Physical Chemistry of Surfaces”, Fifth Edition, John Wiley & Sons, Inc., 1990.

35. Moore, T. F. and Slobod, R. L.: “The Effect of Viscosity and Capillarity on the Displacement of Oil by Water ”, Producers Monthly, 20, pp. 20-30, August 1956.
36. Chatzis, I., Morrow, N. R. and Lim H. T.: “Magnitude and Detailed Structure of Residual Oil Saturation”, SPE 10681-PA, 1983.
37. Darcy, H.: “Les Fontaines Publiques de la Ville de Dijon”, Dalmont, Paris, 1856.
38. Bennion, D. B., Thomas, F. B. and Bietz, R. F.: “Hysteretic Relative Permeability Effects and Reservoir Conformance – An Overview”, Hycal Energy Research Laboratories Ltd., 1996.
39. Corey, A. T.: “The Interrelation between Gas and Oil Relative Permeabilities”, Prod. Mon., pp. 19, 38, 1954.
40. Land, C. S.: “Calculation of Imbibition Relative Permeability for Two- and Three-phase Flow from Rock Properties”, Soc. Pet. Eng. J., pp. 149-156, June 1968.
41. Killough, J. E.: “Reservoir Simulation with History-dependent Saturation Functions”, Trans. AIME 261, Page 37-48, 1976.
42. Carlson, F. M.: "Simulation of Relative Permeability Hysteresis to the Non-Wetting Phase," SPE 10157, Presented at the 56th Annual SPE Technical Conference and Exhibition, San Antonio, Oct. 5-7, 1981.
43. Corey, A. T., Rathjens, C. H., Henderson, J. H. and Wyllie, M. R. J.: ”Three-Phase Relative Permeability”, J. Pet. Tech., 8, 3-5; Trans. AIME, 207, pp. 349-351, 1956.
44. Stone, H. L.: “Probability Model for Estimating Three-Phase Relative Permeability”, Trans AIME (JPT), 249, pp. 214-218, 1970.
45. Stone, H. L.: “Estimation of Three-Phase Relative Permeability and Residual Oil Data”, Can. Pet. Tech., 12, pp. 53-61, 1973.
46. Dietrich, J. K. and Bondor, P. L.: “Three-Phase Oil Relative Permeability Models”, SPE6044, Proceedings of the SPE Annual Conference and Exhibition, New Orleans, LA, October 1976.

47. Aziz, K. and Settari, A.: “Petroleum Reservoir Simulation”, Applied Science Publishers Ltd, London, 1979.
48. Fayers, F. J. and Matthews, J. D.: “Evaluation of Normalized Stone's Methods for Estimating Three-Phase Relative Permeabilities,” SPEJ 224; Trans., AIME, 277, April 1984.
49. Alemán, M. A. and Slattery, J. C.: “Estimation of three-phase relative permeabilities”, Transport in Porous Media, 1988.
50. Baker, L. E.: “Three-Phase Relative Permeability Correlations”, SPE17369, Proceedings of the 1988 Sixth SPE/DOE Symposium on Enhanced Oil Recovery, Tulsa, OK, April 1988.
51. Maini, B. B., Kokal, S. and Jha, K.: “Measurements and Correlations of Three-Phase Relative Permeability at Elevated Temperatures and Pressures”, SPE Annual Technical Conference and Exhibition, San Antonio, Texas, 8-11 October, 1989.
52. Hustad, O. S. and Hansen, A. G.: “A Consistent Formulation for Three-Phase Relative Permeabilities and Phase Pressures Based on Three Sets of Two-Phase Data”, in RUTH: A Norwegian Research Program on Improved Oil Recovery - Program Summary, S.M. Skjaeveland, A. Skauge and L. Hinderacker (Eds.), Norwegian Petroleum Directorate, Stavanger, 1996.
53. Balbinski, E. F., Fishlock, T. P., Goodyear, S. G. and Jones, P. I. R.:”Key Characteristics of Three-Phase Oil Relative Permeability Formulations for Improved Oil Recovery Predictions”, Proceedings of the 9th European Symposium on Improved Oil Recovery, The Hague, October 1997.
54. Moulu, J-C., Vizika, O., Kalaydjian, F. and Duquerroix, J-P.: “A New Model for Three-Phase Relative Permeabilities Based on a Fractal Representation of the Porous Medium”, SPE 38891-MS, paper for SPE Annual Technical Conference and Exhibition, San Antonio, Texas, 5-8 October, 1997.
55. Moulu, J-C., Vizika, O., Egermann, P. and Kalaydjian, F.: “A New Three-Phase Relative Permeability Model for Various Wettability Conditions”, SPE 56477, proceedings of the SPE Annual Technical Conference and Exhibition, Houston, Texas, October, 1999.

56. Blunt, M. J.: “An Empirical Model for Three-phase Relative Permeability”, SPE56474, Proceedings of the SPE Annual Technical Conference and Exhibition, Houston, TX, October 1999.
57. Honarpour, M., Koederitz, L. and Harvey, A. H.: “Relative Permeability of Petroleum Reservoirs”, CRC Press Inc, Boca Raton, FL, United States, 1986.
58. Delshad, M. and Pope, G. A.: “Comparison of Three-Phase Oil Relative Permeability Models”, Transport in Porous Media, 4, pp. 59-83, 1989.
59. Pejic, D. and Maini, B.: “Three-phase Relative Permeability of Petroleum Reservoirs,” SPE 81021, 2003.
60. Leverett, M. C. and Lewis, M. E.: “Steady flow of gas-oil-water mixtures through unconsolidated sands”, Trans. AIME, 1941.
61. Donaldson, E. C. and Dean, G. W.: “Two- and three-phase relative permeability studies”, technical report, Bureau of Mines, Bartlesville, Oklahoma, 1965.
62. Saraf, D. N., Batycky, J. P., Jackson, J. H. and Fisher, D. B.: “An Experimental Investigation of Three-Phase Flow in Water-Oil-Gas Mixtures through Water-Wet Sandstones”, SPE10761, Proceedings of the SPE Regional Meeting, San Francisco, CA, 1982.
63. Grader, A. S. and O’Meara, D. J.: “Dynamic Displacement Measurements of Three-Phase Relative Permeabilities Using Three Immiscible Liquids”, SPE18293, proceedings of the SPE 63rd Annual Technical Conference and Exhibition, Houston, Texas, October 1988.
64. Oak, M. J.: “Three-Phase Relative Permeability of Water-Wet Berea,” SPE 20183, presented at the 1990 SPE/DOE Seventh Symposium on Enhanced Oil Recovery, Tulsa, 22-25 April, 1990.
65. Oak, M. J., Baker, L. E. and Thomas, D. C.: “Three-Phase Relative Permeability of Berea Sandstone”, J. Pet. Tech., 42, pp. 1054-1061, 1990.
66. Oak, M. J.: “Three-Phase Relative Permeability of Intermediate-Wet Berea Sandstone”, SPE22599, proceedings of the SPE Annual Technical Meeting and Exhibition, Dallas, TX, October 1991.

67. Skauge, A. and Larsen, J. A.: “ Three-Phase Relative Permeabilities and Trapped Gas Measurements Relating to WAG Processes”, proceedings of International Symposium of the Society of Core Analysts, Norway, 12th-14th September 1994.
68. Eleri, O. O., Graue, A. and Skauge, A.: "Calculation of Three-Phase Relative Permeabilities from Displacement Experiments with Measurements of In-situ Saturation", SCA 9507, 1995
69. Eleri, O. O., Graue, A. and Skauge, A.: “Steady-State and Unsteady-State Two Phase Relative Permeability Hysteresis and Measurements of Three Phase Relative Permeabilities using Imaging Techniques”, SPE 30764, proceeding SPE Anual Meeting, 22-25 October 1995.
70. Baker, L. E.: “Three-phase relative permeability of water-wet, intermediate-wet and oil-wet sandstone” Geological Society London, Special Publications, v. 84, pp. 51-61, 1995
71. Nordtvedt, J. E., Ebeltoft, E., Iversen, J. E., Sylte, A., Urkedal, H., Vatne, K. O. and Watson, A. T.: “Determination of Three-phase Relative Permeabilities from Displacement Experiments”, SPE36683, proceedings of the SPE Annual Technical Conference and Exhibition, Denver, Colorado, October 1996.
72. Larsen, J. A. and Skauge, A.: "Methodology for Numerical Simulation with Cycle-Dependent Relative Permeabilities", Society of Petroleum Engineers Journal, 163-73, June 1998.
73. Egermann, P., Vizika, O., Dallet, L., Requin, C. and Sonier, F.: ”Hysteresis in Three-Phase Flow: Experiments, Modeling and Reservoir Simulations,” SPE 65127-MS, paper for the SPE European Petroleum Conference, Paris, France, 24-25 October, 2000.
74. Heiba, A. A., Davis, H. T. and Scriven, L. E.: “Statistical Network Theory of Three-Phase Relative Permeabilities”, SPE12690, proceedings of the 4th DOE/SPE Symposium on Enhanced Oil Recovery, Tulsa, Oklahoma, 15-18 April 1984.

75. Fenwick, D. H. and Blunt, M. J.: “Calculating Three-Phase Relative Permeabilities Using Network Modelling“, proceedings of the 5th European Conference on the Mathematics of Oil Recovery, Leoben, Austria, September 1996.
76. Fenwick, D. H. and Blunt, M. J.: “The Use of Network Modelling to Predict Saturation Paths, Relative Permeabilities and Oil Recovery for Three-Phase Flow in Porous Media“, SPE38881, proceedings of the SPE Annual Technical Conference and Exhibition, San Antonio, Texas, October 1997.
77. Fenwick, D. H. and Blunt, M. J.: “Three-Dimensional Modelling of Three-Phase Imbibition and Drainage “, Adv. in Water Resources, 25, pp. 121-143, 1998.
78. Fenwick, D. H. and Blunt, M. J.: “Network Modeling of Three-Phase Flow in Porous Media”, SPE38881, SPE Journal, Volume 3, Number 1, pp. 86-96, March 1998.
79. van Dijke, M. I. J., Sorbie, K. S. and McDougall, S. R.: “A Process-Based Approach for Three-Phase Capillary Pressure and Relative Permeability Relationships in Mixed-Wet Systems”, SPE 59310, paper for SPE/DOE Conference on Improved Oil Recovery, Tulsa, Oklahoma, 3-5 April, 2000.
80. Øren, P. E., Bakke, S. and Arntzen, O. J.: “Extending predictive capabilities to network models”, SPE J, 3, pp. 324-336, 1998.
81. Lerdahl, T. R., Øren, P. E. and Bakke, S.: “A Predictive Network Model for Three-Phase Flow in Porous Media”, SPE59311, proceedings of the SPE/DOE Conference on Improved Oil Recovery, Tulsa, Oklahoma, 3-5 April, 2000.
82. Piri, M. and Blunt, M. J.: “Pore-Scale Modelling of Three-Phase Flow in Mixed-Wet Systems”, SPE 77726, proceedings of the SPE Annual Technical Conference and Exhibition, San Antonio, October 2002.
83. Piri, M. and Blunt M. J.: “Three-dimensional mixed-wet pore-scale network modeling of two- and three-phase flow in porous media. II. Results”. Phys. Rev. E. 71, 026302, 2005.

84. van Dijke, M. I. J., McDougall, S. R. and Sorbie, K. S.: "Three Phase Capillary Pressure and Relative Permeability Relationships in Mixed-Wet Systems", Transport in Porous Media, 44,pp.1-32, 2001
85. van Dijke, M. I. J., Sorbie, K. S. and McDougall, S. R.: “Saturation-Dependencies of Three-Phase Relative Permeabilities in Mixed-wet and Fractionally-Wet Systems”, Adv. Water Resour., 24, 365-384, 2001.
86. van Dijke, M. I. J. and Sorbie, K. S.: 2002, “Pore-Scale Network Model for Three-Phase Flow in Mixed-Wet Porous Media”, Phys. Rev. E., 66, 046302, 2002.
87. Svirsky, D. S., van Dijke, M. I. J. and Sorbie, K. S. “Prediction of Three-Phase Relative Permeabilities Using a Pore-Scale Network Model Anchored to Two-Phase Data“, presented at the SPE Annual Technical Conference and Exhibition, Houston, Texas, 26-29 September 2004.
88. McDougall, S. R., Cruickshank J. and Sorbie K. S.: “Anchoring Methodologies for Pore-Scale Network Models: Application to Relative Permeability and Capillary Pressure Prediction”, proceedings of 2001 International Symposium of the Society of Core Analysts, Edinburgh, 2001.
89. Sorbie, K. S. and van Dijke, M. I. J.: “Fundamentals of Three-Phase Flow in Porous Media of Heterogeneous Wettability”, report, Department of Petroleum Engineering, Heriot-Watt University, May 2001.
90. Eclipse simulation software manual 2006.1, Reference manual, Schlumberger.
91. Kossack, C. A.: “ECLIPSE Users How to Guide for Hysteresis: The Effect of Hysteresis Options in Eclipse”, Schlumberger Holditch-Reservoir Technologies Publication, Denver, 1999.
92. Holmgren, C. R. and Morse, R. A.: “Effect of Free Gas Saturation on Oil Recovery by Water Flooding”, Pet. Trans. AIME 192, 135-140, 1951.
93. Skauge, A. and Aarra, M.: "Effect of Wettability on the Oil Recovery by WAG", presented at the 7th European IOR-Symposium in Moscow, proceedings Vol 2, pp. 452-458, Oct. 26-28, 1993.

94. Skauge, A.: “Summary of Core Flood Results in Connection with WAG Evaluation”, proceedings, the Tenth Wyoming Enhanced Oil Recovery Symposium, University of Wyoming, Laramie, Wyoming, Sept. 20, 1994.
95. Skauge, A. and Larsen, J. A.: “Three-Phase Relative Permeabilities and Trapped Gas Measurements Related to WAG Processes," SCA 9421, presented at the International Symposium of the Society of Core Analysts, Stavanger, proceeding paper Society of Core Analysts, Sept. 12-14, 1994.
96. Ma, T. D. and Youngren, G. K.: “Performance of Immiscible Water-Alternating-Gas (IWAG) Injection at Kuparuk River Unit, North Slope, Alaska”, SPE 28602, presented at the 69th ATCE symposium, New Orleans, 1994.
97. Jerauld, G. R.: “Gas-Oil Relative Permeability of Prudhoe Bay”, SPE 35718, presented at the Western Regional Meeting, Anchorage, 1996.
98. Kyte, J. R., Stanclift, R. J. Jr., Stephan, S. C. Jr. and Rapoport L. A.: “Mechanism of Water Flooding in the Presence of Free Gas”, Pet. Trans. AIME 207, 215-221, 1956.
99. Kortekaas, T.F.M. and van Poelgeest, F.: "Liberation of Solution Gas during Pressure Depletion of Virgin and Watered-out Oil Reservoirs", SPE19693, SPERE, Volume 6, Number 3, pp. 329-335, Aug. 1991.
100. Skauge, A.: "Influence of Wettability on Trapped Non-Wetting Phase Saturation in Three-Phase Flow," proceedings Fourth International Symposium on Wettability and it's Effect on Oil Recovery, Montpellier, France, Sept. 1996.
101. Kralik, J. G., Manak, L. J., Jerauld, G. R. and Spence, S. P.: “Effect of Trapped Gas on Relative Permeability and Residual Oil Saturation in Oil-Wet Sandstone”, SPE 62997, presented at the 75th ATCE symposium, Dallas, 2000.
102. Skauge, A. and Ottesen, B.: “A Summary of Experimentally Derived Relative Permeability and Residual Saturation on North Sea Reservoir Cores”, SCA 2002-12, 2002.

103. Caubit, C., Bertin, H. and Hamon, G.: “Three-Phase Flow in Porous Media: Wettability Effect on Residual Oil Saturation during Gravity Drainage and Tertiary Waterflood”, SPE 90099, presented at the ATCE symposium, Houston, 2004.
104. Maloney, D. and Zornes, D.: “Trapped Versus Initial Gas Saturation Trends from a Single Core Test”, SCA 2003-22, 2002.
105. Johnson, E.F., Bossler, D.P. and Naumann, V.O.: “Calculation of relative permeability from displacement experiments,” Trans. AIME 216, 370, 1959
106. Craig, Jr. F.F.: The reservoir engineering aspects of waterflooding, SPE of AIME, 1971, 23
107. Honarpour, M., Koederitz, L. and Harvey, A.H.: Relative permeability of petroleum reservoirs, CRC Press inc., Boca Raton 1986, (1-5)
108. Vignes, O.: “Application of Optimization Methods in Oil Recovery Problems,” Ph.D. thesis, U. of Trondheim, 1993.
109. Skauge, A., Håskjold, G.S., Thorsen, T. and Aarra, M.G.: "Accuracy of gas - oil relative permeability from two-phase flow experiments," proceedings from Society of Core Analysts, SCA, Calgary, Sept. 1997.
110. Stone, H. L.: “Vertical Conformance in an Alternating water-Miscible Gas Flood”, SPE 11130, presented at the SPE Annual Technical Meeting and Exhibition, New Orleans, 26-29 September 1982.
111. Jenkins, M. K.: “An Analytical Model for Water/Gas Miscible Displacement”, SPE 12632, presented at the SPE/DOE Symposium on Enhanced Oil Recovery, Tulsa, 15-18 April 1984.
112. Skauge, A. and Larsen, J. A.: “New Approach to Model the WAG process”, proceedings 15th International Energy Agency Collaborative Project on Enhanced Oil Recovery, Workshop and Symposium, Bergen, Norway, 28-31 August 1994.
113. Skauge, A. and Larsen, J. A.: “Comparing Hysteresis Models for Relative Permeability in WAG Studies”, SCA 9507, Society of Core Analysts, September 12-14 1995.

114. Skauge, A.; “Simulation studies of WAG using three-phase relative permeability hysteresis models”, paper number 015, proceeding from EAGE 9th European Symposium on Improved Oil Recovery, The Hague, 20-22 October 1997.
115. Skauge, A. and Berg, E.: “Immiscible WAG Injection in the Fensfjord Formation of the Brage Oil Field”, paper 014, proceeding from EAGE, 9th European Symposium on Improved Oil Recovery, The Hague, 20-22 October 1997.
116. Larsen J. A. and Skauge, A.: “Simulation of the Immiscible WAG Process using Cycle-Dependent Three-Phase Relative Permeabilities”, SPE 56475, Society of Petroleum Engineers, ATC&E, 3-6 October 1999.
117. Fatt, I.: “The network model of porous media I. Capillary pressure characteristics.”, Trans AIME, 207, pp. 144-159, 1956.
118. Fatt, I.: “The network model of porous media II. Dynamic properties of a single size tube network.”, Trans AIME, 207, pp. 160-163, 1956.
119. Fatt, I.: “The network model of porous media III. Dynamic properties of networks with tube radius distribution.”, Trans AIME, 207, pp. 164-181, 1956.
120. Koplik, J.: “Creeping flow in two-dimensional networks”, J. Fluid Mech., 119, pp. 219-247, 1982.
121. Wilkinson, D. and Willemsen, J. F.: “Invasion percolation: a new form of percolation theory”, J. Phys. A., 16, pp. 3365-3370, 1983.
122. Stauffer D. and Aharony, A.: “Introduction to Percolation Theory”, 2nd Edition, Taylor & Francis, London, 1992.

Nomenclature

A	cross section area
a_o	constant in the Corey type and Skjæveland et. al correlation
a_w	constant in the Corey type and Skjæveland et. al correlation
C	constant in the Corey correlation and Land correlation
c_o	constant in the Skjæveland et. al correlation
$C_{s,o}$	spreading coefficient
c_w	constant in the Skjæveland et. al correlation
dP	differential pressure
dx	differential distance
E	curvature parameter
F	factor in Killough's correlation
F_{down}	downward force
F_{up}	upward force
g	gravity acceleration and conductance
h	height
k	permeability
k_i	effective permeability for fluid i
k_{rg}	relative permeability for gas
k_{ri}	relative permeability for fluid i
k_{ro}	relative permeability for oil
k_{rog}	two-phase oil relative permeability in a gas-oil system

k_{row}	two-phase oil relative permeability in a oil-water system
k_{rw}	relative permeability for water
$(k_{rg})_{S_{orwg}}$	water relative permeability at residual oil saturation after gas injection
$(k_{ro})_{S_{gc}}$	oil relative permeability at critical gas saturation
$(k_{ro})_{S_{wi}}$	oil relative permeability at irreducible water saturation
$(k_{rw})_{S_{orwc}}$	water relative permeability at residual oil saturation after water injection
$k_{rg}^{2-phase,go}$	gas relative permeability for the 2-phase gas-oil case
$k_{rg}^{2-phase,gw}$	gas relative permeability for the 2-phase gas-water case
$k_{ro}^{2-phase,go}$	oil relative permeability for the 2-phase gas-oil case
$k_{ro}^{2-phase,ow}$	oil relative permeability for the 2-phase oil-water case
$k_{rw}^{2-phase,gw}$	water relative permeability for the 2-phase gas-water case
$k_{rw}^{2-phase,ow}$	water relative permeability for the 2-phase oil-water case
n_g	gas relative permeability exponent
n_{og}	oil relative permeability exponent in presence of gas
n_{ow}	oil relative permeability exponent in presence of water
n_w	gas relative permeability exponent
P_C	capillary pressure
$P_{C,aw}$	capillary pressure between air and water
P_{Cd}	drainage capillary pressure
$P_{C,entry}$	capillary entry pressure
P_{Cgo}	gas-oil capillary pressure

P_{Cgw}	gas-water capillary pressure
$P_{C\,i}$	imbibition capillary pressure
P_{Cow}	oil-water capillary pressure
$P_{Cgo}^{2-phase}$	gas-oil capillary pressure for 2-phase
$P_{Cgw}^{2-phase}$	gas-water capillary pressure for 2-phase
$P_{Cow}^{2-phase}$	oil-water capillary pressure for 2-phase
P_e	capillary entry pressure
$P_{entry,w}$	capillary entry pressure for water wet pores
$P_{non-wetting}$	pressure in non-wetting phase
P_{oil}	pressure in oil
P_{water}	pressure in water
$P_{wetting}$	pressure in wetting phase
q	flow rate
R	radius and residual oil reduction factor
r	radius
$R_{\max}$	maximum radius
$r_{\max}$	maximum radius
$R_{\min}$	minimum radius
$r_{\min}$	minimum radius
$r_{\max}^{\ o}$	maximum radius for oil wet pores
$r_{\min}^{\ w}$	minimum radius for water wet pores
r_p	radius pore

r_t	radius throat
r_{wet}^{o}	radius for oil wet pores near wettability change
r_{wet}^{w}	radius for water wet pores near wettability change
S_e	effective saturation
S_g	gas saturation
S_g^*	effective gas saturation
S_{gc}	critical gas saturation
S_{gi}	initial gas saturation
S_{gt}	trapped gas saturation
S_{lc}	total critical liquid saturation given as
$S_{nw,\max}$	maximum saturation of the non-wetting fluid
$S_{nw,t}$	trapped saturation of the non-wetting fluid
S_o	oil saturation
S_o^*	effective oil saturation
S_{or}	residual oil saturation
S_{org}	residual oil saturation after gas injection
S_{orm}	minimum residual oil saturation
S_{orw}	residual oil saturation after water injection
S_w	water saturation
S_w^*	effective water saturation
$S_{w,hys}$	water saturation at the hysteresis reversal point

S_{wi}	irreducible water saturation
$S_{w,\max}$	maximum water saturation attainable on the scanning curve
V	volume
β_g	gas factor in the Stone I correlation
β_w	water factor in the Stone I correlation
$\Delta\rho$	difference in density
θ_a	advancing contact angle
θ_{aw}	angle between the air-water interface and solid
θ_{go}	contact angle gas-oil
θ_{gw}	contact angle gas-water
θ_{ow}	contact angle oil-water
θ_r	receding contact angle
λ	pore size index and conductance exponent
μ	viscosity
ν	volume exponent
π	constant approximately 3.14
ρ_a	density of air
ρ_w	density of water
σ	interfacial tension
σ_{aw}	interfacial tension between air and water
σ_{go}	interfacial tension between the gas and oil
σ_{gs}	interfacial tension between the gas and solid

σ_{gw}	interfacial tension between the gas and water
σ_{os}	interfacial tension between the oil and solid
σ_{ow}	interfacial tension between oil and water
σ_{ws}	interfacial tension between the water and solid